

# Capacity and Plasticity of Potassium Channels and High-Affinity Transporters in Roots of Barley and Arabidopsis<sup>1[C][W]</sup>

Devrim Coskun, Dev T. Britto, Mingyuan Li, Saehong Oh, and Herbert J. Kronzucker\*

Department of Biological Sciences, University of Toronto, Toronto, Ontario, Canada M1C 1A4

The role of potassium ( $K^+$ ) transporters in high- and low-affinity  $K^+$  uptake was examined in roots of intact barley (*Hordeum vulgare*) and Arabidopsis (*Arabidopsis thaliana*) plants by use of  $^{42}K$  radiotracing, electrophysiology, pharmacology, and mutant analysis. Comparisons were made between results from barley and five genotypes of Arabidopsis, including single and double knockout mutants for the high-affinity transporter, AtHAK5, and the Shaker-type channel, AtAKT1. In Arabidopsis, steady-state  $K^+$  influx at low external  $K^+$  concentration ( $[K^+]_{ext} = 22.5 \mu M$ ) was predominantly mediated by AtAKT1 when high-affinity transport was inhibited by ammonium, whereas in barley, by contrast,  $K^+$  channels could not operate below  $100 \mu M$ . Withdrawal of ammonium resulted in an immediate and dramatic stimulation of  $K^+$  influx in barley, indicating a shift from active to passive  $K^+$  uptake at low  $[K^+]_{ext}$  and yielding fluxes as high as  $36 \mu mol g$  (root fresh weight) $^{-1} h^{-1}$  at  $5 mM [K^+]_{ext}$ , among the highest transporter-mediated  $K^+$  fluxes hitherto reported. This ammonium-withdrawal effect was also established in all Arabidopsis lines (the wild types, *atakt1*, *athak5*, and *athak5 atakt1*) at low  $[K^+]_{ext}$ , revealing the concerted involvement of several transport systems. The ammonium-withdrawal effect coincided with a suppression of  $K^+$  efflux and a significant hyperpolarization of the plasma membrane in all genotypes except *athak5 atakt1*, could be sustained over 24 h, and resulted in increased tissue  $K^+$  accumulation. We discuss key differences and similarities in  $K^+$  acquisition between two important model systems and reveal novel aspects of  $K^+$  transport in planta.

Potassium ( $K^+$ ), a major macronutrient in plants, is the most abundant intracellular cation (constituting up to 10% of plant dry weight) and is critical to such cellular functions as osmotic balance, enzyme activation, and electrical regulation (Leigh and Wyn-Jones, 1984; Maathuis and Sanders, 1996; Britto and Kronzucker, 2008). Understanding the mechanisms of  $K^+$  acquisition in plants has long been of scientific and practical importance and is increasingly urgent in light of major ecological and agricultural problems, such as soil  $K^+$  level decline (Ashley et al., 2006, and refs. therein) and sodium ( $Na^+$ ) and ammonium ( $NH_4^+$ ) toxicities (Britto and Kronzucker, 2002; Kronzucker et al., 2006; ten Hoopen et al., 2010).

Since the pioneering work of Epstein et al. (1963), which described the acquisition of  $K^+$  by plants as the sum of activities of two transport systems with distinct substrate-binding affinities, major advances in the molecular and thermodynamic characterization of each system have

been made (for review, see Maathuis and Sanders, 1996; Véry and Sentenac, 2003; Britto and Kronzucker, 2008; Szczerba et al., 2009). Generally, Epstein's mechanism 1, or the high-affinity transport system (HATS), has been described as a saturable system that catalyzes the thermodynamically active uptake (i.e. ATP-dependent transport against an electrochemical gradient) of  $K^+$  from external concentrations ( $[K^+]_{ext}$ ) of less than  $1 mM$  (Kochian and Lucas, 1982; Maathuis and Sanders, 1994). Mechanism 2, or the low-affinity transport system (LATS), catalyzes a flux proportional to  $[K^+]_{ext}$  and is proposed to predominate above  $1 mM [K^+]_{ext}$  (Epstein et al., 1963; Kochian et al., 1985; Maathuis and Sanders, 1996). Although several molecular candidates have been suggested to encode HATS and LATS proteins (Szczerba et al., 2009), it is believed that the majority of high-affinity transport is catalyzed by secondary active transporters of the HAK/KUP/KT family (e.g. AtHAK5 from Arabidopsis [*Arabidopsis thaliana*] and HvHAK1 from barley [*Hordeum vulgare*]), which operate via a proton ( $H^+$ )/ $K^+$  symport mechanism (Gierth and Mäser, 2007). Low-affinity transport, by contrast, occurs via Shaker-like  $K^+$  channels (e.g. AtAKT1 from Arabidopsis and HvAKT1 from barley), which facilitate passive diffusion down the electrochemical gradient for  $K^+$  (Véry and Sentenac, 2003; Chérel, 2004). Other key transporters implicated in  $K^+$  uptake include nonselective cation channels (NSCCs; Demidchik et al., 2002) and HKT/TRK-type transporters (Rubio et al., 1995). An unidentified system in Arabidopsis, independent of AtAKT1 and AtHAK5 and reportedly operating only at high (millimolar)  $[K^+]_{ext}$ , has

<sup>1</sup> This work was supported by the Natural Sciences and Engineering Research Council of Canada, the Canada Research Chair program, and the Canadian Foundation for Innovation.

\* Corresponding author; e-mail herbertk@utsc.utoronto.ca.

The author responsible for distribution of materials integral to the findings presented in this article in accordance with the policy described in the Instructions for Authors ([www.plantphysiol.org](http://www.plantphysiol.org)) is: Herbert J. Kronzucker (herbertk@utsc.utoronto.ca).

[C] Some figures in this article are displayed in color online but in black and white in the print edition.

[W] The online version of this article contains Web-only data.

[www.plantphysiol.org/cgi/doi/10.1104/pp.113.215913](http://www.plantphysiol.org/cgi/doi/10.1104/pp.113.215913)

been the subject of considerable recent interest (Pyo et al., 2010; Rubio et al., 2010; Caballero et al., 2012; see also Hirsch et al., 1998); however, little is known about its molecular and physiological characterization.

The nutritional and molecular regulation of HAK/KUP/KT transporters and Shaker-like  $K^+$  channels has been extensively investigated in the model system *Arabidopsis* and has led to some blurring of distinctions between the traditional concepts of HATS and LATS (Spalding et al., 1999; Xu et al., 2006; Lee et al., 2007; Qi et al., 2008; Geiger et al., 2009; Honsbein et al., 2009; Pyo et al., 2010; Rubio et al., 2010; for review, see Alemán et al., 2011). For instance, although HAK/KUP/KT transporters appear to dominate the HATS (Gierth and Mäser, 2007), some members have been demonstrated to operate at  $[K^+]_{ext}$  as high as 20 mM, indicating a dual affinity (Fu and Luan, 1998; Kim et al., 1998). By contrast, although generally ascribed to the LATS (Maathuis and Sanders, 1996), AtAKT1 can operate at  $[K^+]_{ext}$  as low as 10  $\mu$ M, given favorable thermodynamic conditions, and particularly if the HATS is suppressed by  $NH_4^+$  (Hirsch et al., 1998; Spalding et al., 1999), which specifically inhibits HAK/KUP/KT transporters (Qi et al., 2008). Further blurring the distinction between HATS and LATS is the response of  $K^+$  uptake mechanisms to  $K^+$  limitation (Hampton et al., 2004). For instance, HAK/KUP/KT expression (Ahn et al., 2004; Gierth et al., 2005) and high-affinity  $K^+$  influx (Glass, 1976; Kochian and Lucas, 1982; Siddiqi and Glass, 1986) have both been shown to be up-regulated by  $K^+$  starvation. On the other hand, while AtAKT1 expression appears to be independent of  $K^+$  availability (Lagarde et al., 1996; Gierth et al., 2005), the posttranslational regulation of AtAKT1 (including phosphorylation/dephosphorylation networks and channel heteromerization) has shown that channel-mediated  $K^+$  uptake can increase in response to low- $K^+$  conditions (Li et al., 2006; Xu et al., 2006; Lee et al., 2007; Geiger et al., 2009; Grefen et al., 2010; Jeanguenin et al., 2011).

While much recent work on  $K^+$  uptake has occurred in *Arabidopsis*, leading to the development of a sophisticated model (Alemán et al., 2011), little attention has been given to the question of how general this model might be, most importantly with respect to crop species. This is naturally the result of the vast catalog of well-characterized *Arabidopsis* mutant lines (e.g. The *Arabidopsis* Information Resource [<http://www.arabidopsis.org>] and the *Arabidopsis* Biological Resource Center [<http://abrc.osu.edu>]), which have no equivalent in crop species such as rice (*Oryza sativa*; Goff et al., 2002; Yu et al., 2002; see also Amrutha et al., 2007), barley (Mayer et al., 2012), and wheat (*Triticum aestivum*; Brenchley et al., 2012). Examinations into the molecular identity and contribution of  $K^+$  uptake systems in roots of barley have been limited to high-affinity concentrations (0.1–1 mM), with particular focus on the AtHAK5 homolog, HvHAK1, and its regulation (Santa-María et al., 2000; Vallejo et al., 2005; Fulgenzi et al., 2008). This work indicates that, like *Arabidopsis* (Hirsch et al., 1998; Spalding et al., 1999), high-affinity  $K^+$  uptake in roots of barley is

dictated by  $NH_4^+$ -sensitive and -insensitive systems, linked to HvHAK1 and, most likely, HvAKT1, respectively (Santa-María et al., 2000). However, it has not been explored whether, under high  $NH_4^+$  conditions,  $K^+$  channels can operate in roots of barley at very low  $[K^+]_{ext}$  (e.g. 10  $\mu$ M), as they do in *Arabidopsis* (Hirsch et al., 1998); this information can help address some long-standing speculation on the role of  $K^+$  channels under nutrient deficiency (Kochian and Lucas, 1993). Moreover, the relative apportionment of  $K^+$  channels and secondary active transporters with respect to high- and low-affinity uptake in roots of barley has not been explored to the same extent as in *Arabidopsis* (Rubio et al., 2008, 2010). Lastly, although the inhibition of high-affinity  $K^+$  influx by external  $NH_4^+$  supply is well documented (Vale et al., 1987; Spalding et al., 1999; Santa-María et al., 2000; Qi et al., 2008), as are its effects on membrane polarization (Ullrich et al., 1984; Wang et al., 1994; Britto et al., 2001), little is known about the recovery of  $K^+$  influx and the thermodynamic response following  $NH_4^+$  removal under high- and low-affinity systems. As one of the chief aspects of  $NH_4^+$  toxicity in higher plants, understanding the inhibitory role of this nitrogen source in  $K^+$  transport is of particular importance (Britto and Kronzucker, 2002).

Here, we address these gaps in understanding by providing, to our knowledge, the first in-depth physiological examination of the contribution of  $K^+$  channels and high-affinity transporters to  $K^+$  acquisition in barley. In particular, we posed the following questions. What is the relative apportionment of  $K^+$  channels and high-affinity transporters to high- and low-affinity  $K^+$  uptake in the presence of  $NH_4^+$  in barley, and how does it differ from the *Arabidopsis* model? What are the maximal rates of high- and low-affinity  $K^+$  fluxes in planta? How does  $K^+$  uptake respond to  $NH_4^+$  withdrawal, and what mechanisms underlie this response? With the use of  $^{42}K^+$  radiolabeling, coupled with mutant and electrophysiological analyses, we show that  $K^+$  acquisition at low (22.5  $\mu$ M)  $[K^+]_{ext}$  in the presence of high (millimolar)  $NH_4^+$ , is fundamentally different in the two model systems, chiefly in that  $K^+$  channels operate at such low  $[K^+]_{ext}$  in *Arabidopsis* but not in barley. However, we show that with sudden withdrawal of external  $NH_4^+$ , dramatic shifts in thermodynamic gradients and  $K^+$  fluxes can occur, revealing novel aspects of transport capacity and plasticity. We also provide, to our knowledge, the first in planta  $^{42}K$  examination of the *athak5 atakt1* double mutant, revealing novel aspects of an uptake system as yet unidentified by genetic means.

## RESULTS

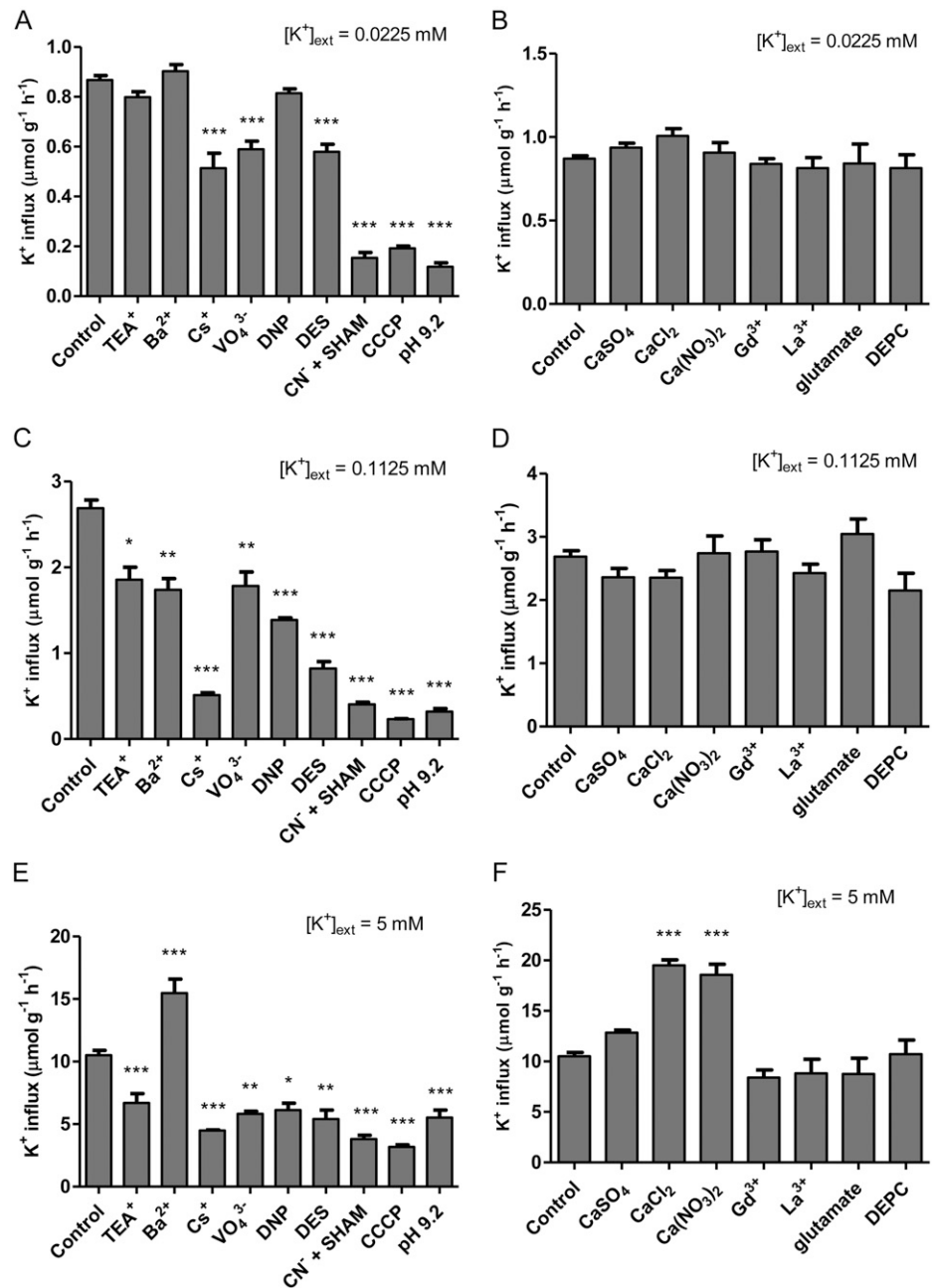
### The Relative Apportionment of $K^+$ Channels and High-Affinity Transporters Differs between Barley and *Arabidopsis* under Steady-State Conditions

Figure 1 shows the results of an extensive pharmacological profiling of steady-state  $K^+$  influx, targeting either Shaker-like  $K^+$  channels and HAK/KUP/KT transporters

(Fig. 1, A, C, and E) or NSCCs (Fig. 1, B, D, and F), in barley grown and tested under high (10 mM)  $\text{NH}_4^+$  and three levels of  $[\text{K}^+]_{\text{ext}}$ : 0.0225 mM (low), 0.1125 mM (intermediate), and 5 mM (high).  $\text{K}^+$  influx was insensitive to the standard  $\text{K}^+$  channel inhibitors, tetraethyl ammonium ( $\text{TEA}^+$ ) and  $\text{Ba}^{2+}$  (White and Lemtiri-Chlieh, 1995; Bertl et al., 1997; Hille, 2001), under low- $\text{K}^+$  conditions (Fig. 1A) but showed significant ( $P < 0.05$ ) inhibition at intermediate  $\text{K}^+$  (Fig. 1C). Under high- $\text{K}^+$  conditions, influx was suppressed by  $\text{TEA}^+$  and, surprisingly, stimulated by  $\text{BaCl}_2$  (Fig. 1E), as also observed with 5 mM  $\text{CaCl}_2$  and  $\text{Ca}(\text{NO}_3)_2$  (Fig. 1F).  $\text{Cs}^+$ , a potent inhibitor of both  $\text{K}^+$  channels and high-affinity transporters (Krol

and Trebacz, 2000; White and Broadley, 2000), significantly suppressed  $\text{K}^+$  influx at low, intermediate, and high  $\text{K}^+$ , by 41%, 81%, and 57%, respectively (Fig. 1, A, C, and E). Metabolic inhibitors vanadate ( $\text{VO}_4^{3-}$ ), 2,4-dinitrophenol (DNP), diethylstilbestrol (DES), cyanide ( $\text{CN}^-$ ) + salicylhydroxamic acid (SHAM), carbonyl cyanide *m*-chlorophenyl hydrazone (CCCP), and pH 9.2 (adjusted with NaOH) were all very effective in suppressing  $\text{K}^+$  influx under all  $[\text{K}^+]_{\text{ext}}$  conditions tested, except for DNP at low  $\text{K}^+$  (Fig. 1, A, C, and E). The NSCC inhibitors  $\text{Ca}^{2+}$ ,  $\text{Gd}^{3+}$ ,  $\text{La}^{3+}$ , Glu, and diethylpyrocarbonate (DEPC; White and Lemtiri-Chlieh, 1995; Essah et al., 2003) had no effect on  $\text{K}^+$  influx at any  $[\text{K}^+]_{\text{ext}}$  tested (Fig. 1, B, D, and F). Note that counter-ion

**Figure 1.** The effects of various pharmacological and nutritional treatments, targeting either Shaker-like  $\text{K}^+$  channels and HAK/KUP/KT transporters (A, C, and E) or NSCCs (B, D, and F), on steady-state  $\text{K}^+$  influx in intact roots of barley seedlings grown in full nutrient medium at low (A and B), intermediate (C and D), and high (E and F)  $[\text{K}^+]_{\text{ext}}$  and 10 mM  $[\text{NH}_4^+]_{\text{ext}}$ . Fluxes are indicated on a root fresh weight basis. Asterisks denote different levels of significance between control and treatment pairs (\* $0.01 < P < 0.05$ , \*\* $0.001 < P < 0.01$ , \*\*\* $P < 0.001$ ; one-way ANOVA with Dunnett's multiple comparison post hoc test). Each treatment represents the mean of four to 69 replicates. Error bars indicate SE.



controls for  $\text{VO}_4^{3-}$ ,  $\text{CN}^-$ , Glu, and pH 9.2 treatments were conducted with 10 mM NaCl and showed no response at any  $[\text{K}^+]_{\text{ext}}$  (data not shown).

Table I displays the results of a thermodynamic (Nernstian) analysis for barley based on compartmental analysis by  $^{42}\text{K}^+$  efflux and electrophysiology. Since physiological efflux was confirmed for low- and intermediate- $\text{K}^+$  conditions (Coskun et al., 2010; see below), the methods of compartmental analysis (Lee and Clarkson, 1986; Siddiqi et al., 1991; Kronzucker et al., 1995) were used to estimate cytosolic potassium concentration ( $[\text{K}^+]_{\text{cyt}}$ ), along with unidirectional fluxes and cytosolic half-times of exchange. Based on estimates of  $[\text{K}^+]_{\text{cyt}}$  equilibrium potentials for  $\text{K}^+$  ( $E_{\text{K}^+}$ ) were calculated (see "Materials and Methods") and were found to be more negative than measured membrane potentials ( $\Delta\Psi_{\text{m}}$ ) for epidermal and cortical root cells at both  $\text{K}^+$  conditions (Table I); thus, thermodynamically active  $\text{K}^+$  uptake was predicted. Since physiological efflux was not found under high- $\text{K}^+$  conditions (see below), neither compartmental nor subsequent thermodynamic analyses could be conducted under those conditions. We should note that  $E_{\text{K}^+}$  is only an approximation, as it should use  $\text{K}^+$  activities rather than  $\text{K}^+$  concentrations. However, approximations of cytosolic  $\text{K}^+$  activity coefficients ( $\gamma_{\text{cyt}}$ ) vary widely in the literature (e.g.  $0.72 < \gamma_{\text{cyt}} < 1.29$ ; Kielland, 1937; Robinson and Stokes, 1965; Ling, 1969; Palmer et al., 1978), reflecting a still surprisingly poor understanding of ion sequestration and interaction in the plant cell cytosol (Cheeseman, 2013). When  $\text{K}^+$  activities were estimated according to standard procedures (using  $\gamma_{\text{cyt}} = 0.75$ ; Walker et al., 1996; Cuin et al., 2003), however,  $E_{\text{K}^+}$  still remained negative of  $\Delta\Psi_{\text{m}}$  (data not shown); thus, the principal thermodynamic conclusions of our analysis still hold.

A selective pharmacological profiling of  $\text{K}^+$  influx in *Arabidopsis* (Columbia [Col-0] wild type, Wassilewskija [WS] wild type, *atakt1*, *athak5*, and *athak5 atakt1*) was conducted at low  $\text{K}^+$  and high  $\text{NH}_4^+$  (Fig. 2). Because *Arabidopsis* exhibited  $\text{NH}_4^+$  toxicity at much lower concentrations than barley (data not shown),  $\text{NH}_4^+$  was provided only at 2 mM (compared with 10 mM in barley). Unlike barley, *Arabidopsis* wild-type lines generally displayed  $\text{TEA}^+$  and  $\text{Ba}^{2+}$  sensitivity under low- $\text{K}^+$ , high- $\text{NH}_4^+$  conditions (although it was not statistically significant in the case of  $\text{TEA}^+$  for WS; Fig. 2B). Consistent with their pharmacological targeting (see above),

$\text{TEA}^+$  and  $\text{Ba}^{2+}$  sensitivity was not found in the AtAKT1 knockout lines *atakt1* and *athak5 atakt1* (Fig. 2, C and E). Further confirmation of the involvement of AtAKT1 was provided by the dramatic decrease in steady-state influx in *atakt1* and *athak5 atakt1* lines compared with their respective wild types (59% and 78%, respectively), while influx for *athak5* was essentially equal to the Col-0 wild type and displayed both  $\text{TEA}^+$  and  $\text{Ba}^{2+}$  sensitivity (albeit not statistically significant in the case of  $\text{TEA}^+$ ; Fig. 2D).  $\text{Cs}^+$  significantly suppressed steady-state influx in all lines, including *athak5 atakt1* (Fig. 2, A–D), while pH 9.2 was about as effective as  $\text{Cs}^+$  in all cases except in *athak5 atakt1* (Fig. 2, A–D).  $\text{Ca}^{2+}$  was ineffective at suppressing steady-state influx in all lines (Fig. 2, A–D).

### Mechanism of $\text{K}^+$ Efflux in Barley Differs Based on $[\text{K}^+]_{\text{ext}}$

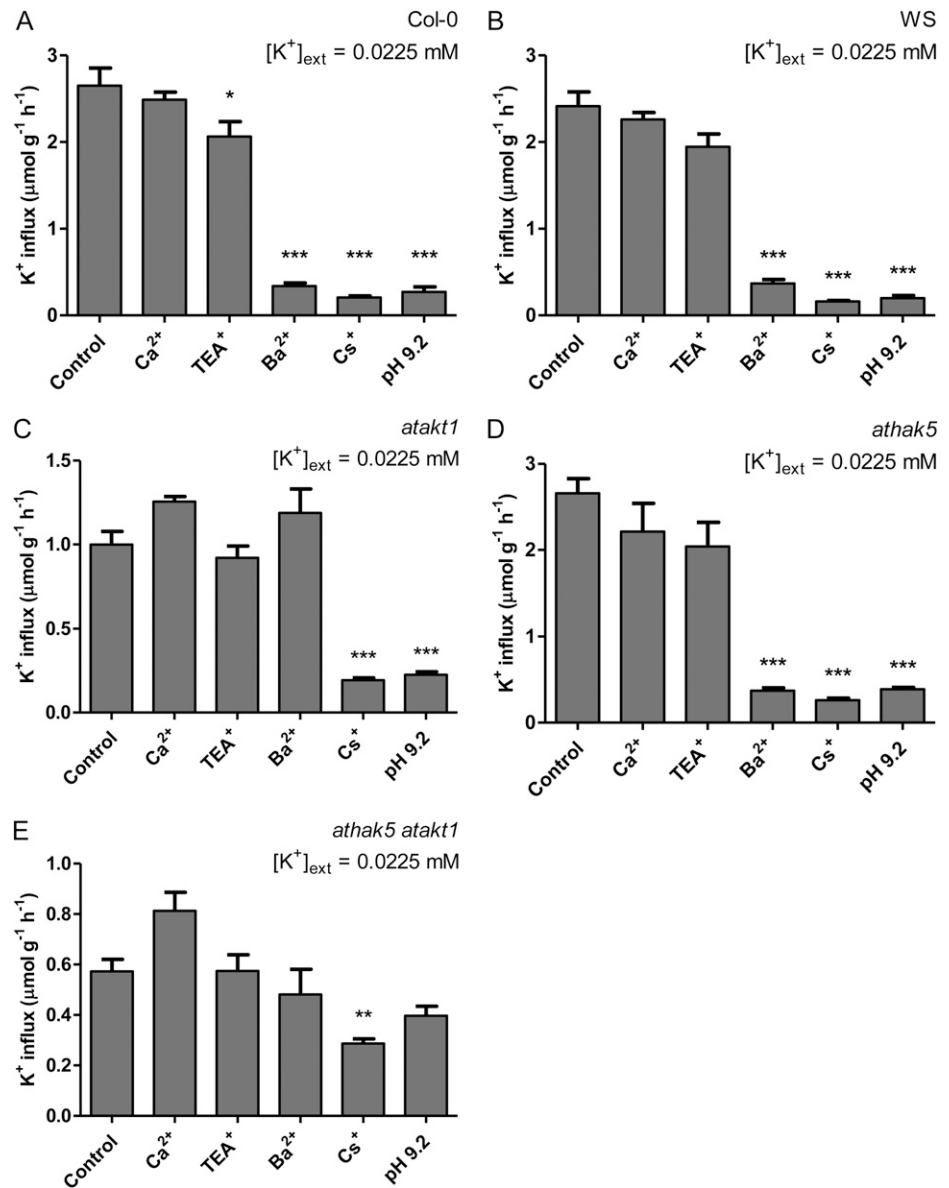
Figure 3 illustrates the pharmacological profiling of steady-state  $\text{K}^+$  efflux in barley under high  $\text{NH}_4^+$  and varying  $[\text{K}^+]_{\text{ext}}$ . Interestingly, at low (22.5  $\mu\text{M}$ )  $[\text{K}^+]_{\text{ext}}$ , application of 10 mM  $\text{Cs}^+$  resulted in an immediate and significant stimulation in  $\text{K}^+$  efflux (Fig. 3A), unlike  $\text{TEA}^+$ ,  $\text{Ba}^{2+}$ , and  $\text{Ca}^{2+}$ , which had no effect. By contrast, at intermediate (112.5  $\mu\text{M}$ )  $[\text{K}^+]_{\text{ext}}$ ,  $\text{Cs}^+$  was effective in inhibiting efflux, as was  $\text{TEA}^+$  (Fig. 3B). At high (5 mM)  $[\text{K}^+]_{\text{ext}}$ ,  $\text{Cs}^+$  showed no effect (Fig. 3C), consistent with the cessation of physiological efflux, which was confirmed by comparing steady-state efflux to pH 9.2 treatments, where roots had been exposed to alkalinity during tracer uptake and elution periods (see "Materials and Methods"). Since pH 9.2 was effective in suppressing influx at all  $[\text{K}^+]_{\text{ext}}$  tested (Fig. 1, A, C, and E), its application during tracer uptake would have inhibited intracellular accumulation. Thus, the significant suppression of tracer release during the slowly exchanging phase in the low- and intermediate- $\text{K}^+$  conditions, and lack thereof at high  $\text{K}^+$  (Fig. 3, insets), with pH 9.2 indicates the cytosolic origin of released tracer at low and intermediate  $\text{K}^+$  and the lack thereof at high  $\text{K}^+$ . Sudden withdrawal of external  $\text{NH}_4^+$  results in a thermodynamic shift (at low and intermediate  $\text{K}^+$ ) and significant stimulations in  $\text{K}^+$  influx (see below), but it was also found to inhibit  $\text{K}^+$  efflux at both  $[\text{K}^+]_{\text{ext}}$  and to cause no effect at high  $\text{K}^+$  (Fig. 3, insets), confirming the proposed dual nature of efflux under high- and low-affinity conditions.

**Table I.** Steady-state  $\text{K}^+$  fluxes, compartmentation, and electrophysiology of intact barley seedling roots

One-week-old barley seedlings were grown on full nutrient medium supplemented with 10 mM  $\text{NH}_4^+$  and either 0.0225 or 0.1125 mM  $\text{K}^+$ .  $\Delta\Psi_{\text{m}}$  measurements were taken from root epidermal and cortical cells 2 to 3 cm from the root tip.  $E_{\text{K}^+}$  and predicted  $[\text{K}^+]_{\text{cyt}}$  were determined with the Nernst equation. Error values indicate SE of six to eight replicates.

$[\text{K}^+]_{\text{ext}}$	Influx	Efflux	Net Flux	Efflux-Influx Ratio	Half-Time	$\Delta\Psi_{\text{m}}$	$E_{\text{K}^+}$	$[\text{K}^+]_{\text{cyt}}$	
								Predicted	Measured
mM		$\mu\text{mol g}^{-1} \text{h}^{-1}$			min	mV		mM	
0.0225	$0.52 \pm 0.03$	$0.27 \pm 0.02$	$0.25 \pm 0.02$	$0.52 \pm 0.03$	$32.90 \pm 2.92$	$-143.6 \pm 2.7$	-153.8	5.57	$8.24 \pm 0.69$
0.1125	$1.89 \pm 0.13$	$0.57 \pm 0.05$	$1.32 \pm 0.10$	$0.30 \pm 0.01$	$32.50 \pm 4.69$	$-136.2 \pm 3.0$	-144.1	20.95	$28.39 \pm 3.40$

**Figure 2.** The effects of various pharmacological and nutritional treatments on steady-state  $K^+$  influx in intact roots of Arabidopsis Col-0 wild type (A), WS wild type (B), *atakt1* (C), *athak5* (D), and *athak5 atakt1* (E) grown in full nutrient medium at low  $[K^+]_{ext}$  and 2 mM  $[NH_4^+]_{ext}$ . Fluxes are indicated on a root fresh weight basis. Asterisks denote different levels of significance between control and treatment pairs (\* $0.01 < P < 0.05$ , \*\* $0.001 < P < 0.01$ , \*\*\* $P < 0.001$ ; one-way ANOVA with Dunnett's multiple comparison post hoc test). Each treatment represents the mean of three to 14 replicates. Error bars indicate se.



### $\text{NH}_4^+$ Withdrawal Results In Thermodynamic Shifts and Significant $K^+$ Influx

$K^+$  influx was stimulated by sudden withdrawal (5-min pretreatment) of  $\text{NH}_4^+$ , by 176%, 355%, and 131% [corresponding to  $2.4 \pm 0.1$ ,  $12.0 \pm 0.4$ , and  $24.3 \pm 0.7 \mu\text{mol g}^{-1} \text{h}^{-1}$ , respectively], at low-, intermediate-, and high- $K^+$  conditions, respectively (Fig. 4).  $\text{NH}_4^+$  withdrawal also led to immediate and significant hyperpolarizations of root epidermal and cortical  $\Delta\Psi_m$  ( $59.1 \pm 13.2$ ,  $53.1 \pm 8.3$ , and  $31.4 \pm 4.9$  mV at low, intermediate, and high  $K^+$ , respectively), corresponding to  $\Delta\Psi_m$  much more negative than  $E_{K^+}$  and, thus, thermodynamic shifts (active to passive influx) at low and intermediate  $K^+$  (Table II; compare with Table I).

This ammonium withdrawal effect (AWE) in barley was also found in Arabidopsis wild-type lines, resulting in 142% and 175% increases in  $K^+$  influx for Col-0

and WS, respectively (Fig. 5, A and B). Interestingly, AWE was also consistently observed in the knockout lines *atakt1* (513%), *athak5* (167%), and *athak5 atakt1* (32% [albeit not statistically significant]; Fig. 5, C–E). As in barley,  $\text{NH}_4^+$  withdrawal also consistently resulted in hyperpolarizations of the plasma membrane of root epidermal and cortical cells in all lines except *athak5 atakt1* (albeit not statistically significant in the cases of WS and *athak5*; Table II).

### $\text{Ca}^{2+}$ Sensitivity of the AWE Depends on $[K^+]_{ext}$ and Genotype

The results of a selective pharmacological profiling of AWE in barley can be seen in Figure 4. Under the three levels of  $[K^+]_{ext}$ , AWE displayed similar inhibitory responses to TEA $^+$ ,  $\text{Ba}^{2+}$ , and  $\text{Cs}^+$  (i.e. TEA $^+$  <  $\text{Ba}^{2+}$  <  $\text{Cs}^+$ ).

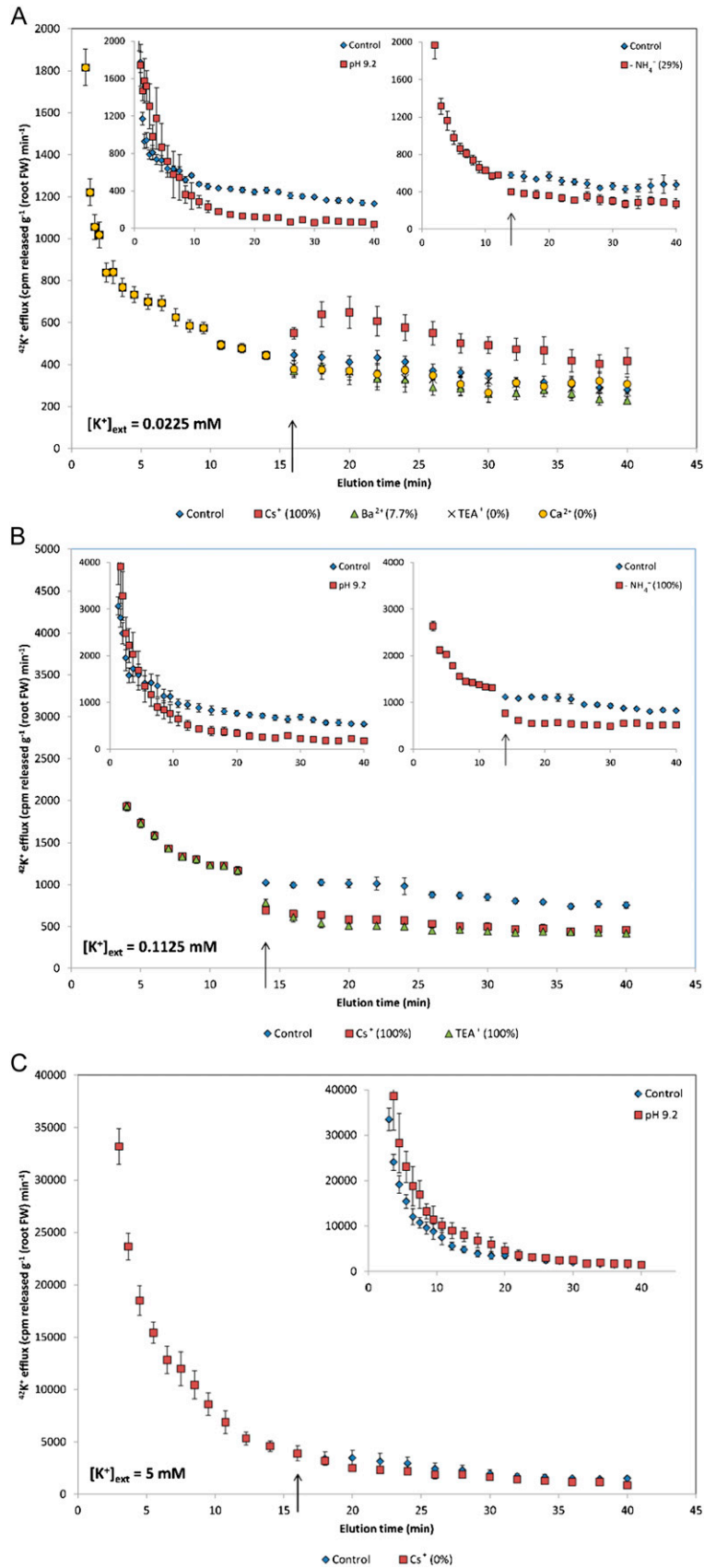
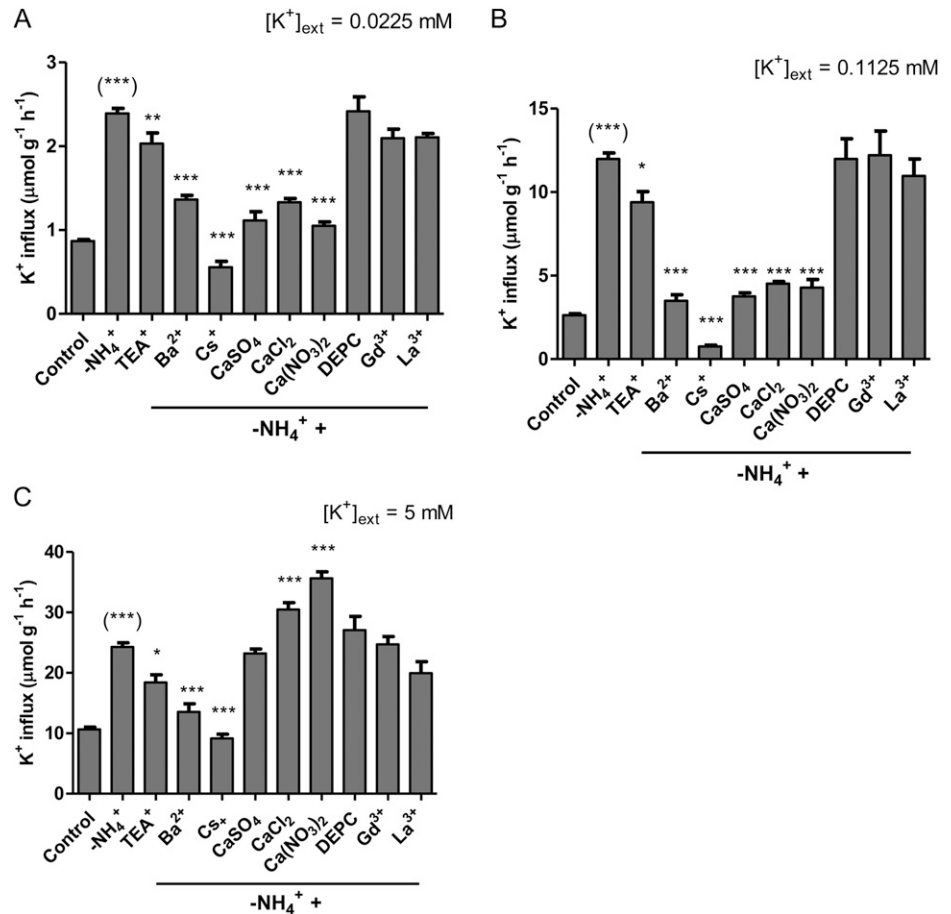


**Figure 3.** Responses of  $^{42}\text{K}^+$  efflux from roots of intact barley seedlings to sudden application (see arrows) of various pharmacological and nutritional treatments. Plants were grown in full nutrient medium at low (A), intermediate (B), and high (C)  $[\text{K}^+]_{\text{ext}}$  and  $10 \text{ mM } [\text{NH}_4^+]_{\text{ext}}$ . Insets show responses of  $\text{K}^+$  efflux to sudden (see arrows) withdrawal of external  $\text{NH}_4^+$  and/or

**Figure 4.** The effects of various pharmacological and nutritional treatments on  $K^+$  influx stimulated due to  $NH_4^+$  withdrawal in intact roots of barley seedlings grown in full nutrient medium at low (A), intermediate (B), and high (C)  $[K^+]_{ext}$  and  $10\text{ mM } [NH_4^+]_{ext}$ . Fluxes are indicated on a root fresh weight basis. Asterisks denote different levels of significance between  $-NH_4^+$  and treatment pairs ( $*0.01 < P < 0.05$ ,  $**0.001 < P < 0.01$ ,  $***P < 0.001$ ; one-way ANOVA with Dunnett's multiple comparison post hoc test). Asterisks in parentheses denote levels of significance between control and  $-NH_4^+$  pairs (Student's  $t$  test). Each treatment represents the mean of four to 69 replicates. Error bars indicate SE.



Interestingly, AWE also displayed significant ( $P < 0.01$ ) inhibition by  $5\text{ mM } Ca^{2+}$  (regardless of the counter ion) at low and intermediate  $K^+$  (Fig. 4, A and B) but not at high  $K^+$  (Fig. 4C). To the contrary, AWE at high  $K^+$  was stimulated by  $Cl^-$  and  $NO_3^-$  (supplied as  $Ca^{2+}$  salts), with the greatest stimulation observed with  $NO_3^-$  [ $36\ \mu\text{mol g (root fresh weight)}^{-1}\text{ h}^{-1}$ ]. AWE showed no response to the NSCC inhibitors DEPC,  $Gd^{3+}$ , and  $La^{3+}$  at any  $[K^+]_{ext}$  (Fig. 4).

The differential response of AWE to  $Ca(NO_3)_2$  under varying  $[K^+]_{ext}$  (i.e. inhibition at low and intermediate  $K^+$ , stimulation at high  $K^+$ ) was also explored electrophysiologically. As shown in Table II, switching from  $(NH_4)_2SO_4$  to equimolar  $Ca(NO_3)_2$  resulted in further hyperpolarizations of the plasma membrane of root epidermal and cortical cells at low and intermediate  $K^+$  compared with  $NH_4^+$  withdrawal alone. By contrast, at high  $K^+$ , this resulted in less hyperpolarization compared with  $NH_4^+$  withdrawal alone.

Similar to barley (at low  $K^+$ ), AWE in Arabidopsis wild-type lines showed comparable responses to  $TEA^+$ ,  $Ba^{2+}$ ,  $Cs^+$ , and  $Ca^{2+}$  (Fig. 5, A and B). This was also

observed in *athak5* (Fig. 5D). As expected, AWE in *atakt1* and *athak5 atakt1* no longer displayed sensitivity to the channel inhibitors  $TEA^+$  and  $Ba^{2+}$  but remained significantly  $Cs^+$  sensitive (Fig. 5, C and E). Surprisingly, however, the  $Ca^{2+}$  sensitivity of AWE was lost in *atakt1* and *athak5 atakt1* (Fig. 5, C and E).

#### AWE over 24 h Reveals Peaks in $K^+$ Influx and Leads to Tissue $K^+$ Accumulation

Figure 6 illustrates the sustainability of AWE (i.e. elevated  $K^+$  influx after ammonium withdrawal) and its magnitude over 24 h at all three  $K^+$  levels in barley. At low  $K^+$ , AWE was not only sustained over 24 h but continued to rise, reaching  $4.2\ \mu\text{mol g (root fresh weight)}^{-1}\text{ h}^{-1}$  (a 4.6-fold increase from control). At intermediate  $K^+$ , AWE plateaued between 8 and 12 h, reaching  $10\ \mu\text{mol g (root fresh weight)}^{-1}\text{ h}^{-1}$  (a 6.8-fold increase from control), before dropping to approximately  $5\ \mu\text{mol g (root fresh weight)}^{-1}\text{ h}^{-1}$  by 24 h. At high  $K^+$ ,  $NH_4^+$  withdrawal peaked at  $25\ \mu\text{mol g (root fresh weight)}^{-1}\text{ h}^{-1}$  by

#### Figure 3. (Continued.)

alkalinity during radiotracer uptake and elution periods. Numbers in parentheses indicate percentages of treated points differing significantly from the control (Student's  $t$  test;  $P < 0.05$ ). In the insets, axis labels are as in the main figures. Each plot represents the mean of three to seven replicates. Error bars indicate SE. FW, Fresh weight. [See online article for color version of this figure.]

**Table II.** Electrophysiological responses of barley and *Arabidopsis* root cells to sudden  $\text{NH}_4^+$  withdrawal with or without  $\text{Ca}(\text{NO}_3)_2$ 

One-week-old barley seedlings and 5-week-old *Arabidopsis* plants were grown on full nutrient medium supplemented with high  $\text{NH}_4^+$  (2 mM in *Arabidopsis*, 10 mM in barley) and 0.0225, 0.1125, or 5 mM  $\text{K}^+$ .  $\Delta\Psi_m$  measurements were taken from root epidermal and cortical cells 2 to 3 cm from the root tip, and the  $\text{AWE} \pm \text{Ca}(\text{NO}_3)_2$  (5 mM in barley) was measured. Letters denote significantly different means ( $P < 0.05$ ; one-way ANOVA with Bonferroni post hoc test), and asterisks denote different levels of significance between control and treatment pairs (\*\*0.001  $< P < 0.01$ ; Student's *t* test); ns, not significant. Error values indicate SE of four replicates. n.d., Not determined.

Species	Genotype	$[\text{K}^+]_{\text{ext}}$	$\Delta\Psi_m$		
			Control	AWE	AWE $\pm$ $\text{Ca}(\text{NO}_3)_2$
		mM		mV	
Barley	Metcalf (wild type)	0.0225	$-143.6 \pm 2.7^a$	$-202.6 \pm 21.7^b$	$-251.4 \pm 13.0^c$
		0.1125	$-136.2 \pm 3.0^a$	$-189.3 \pm 8.9^b$	$-208.5 \pm 10.0^b$
		5	$-133.2 \pm 2.2^a$	$-164.6 \pm 5.1^b$	$-149.0 \pm 8.0^b$
<i>Arabidopsis</i>	Col-0	0.0225	$-165.0 \pm 13.7$	$-231.0 \pm 8.1^{**}$	n.d.
	WS		$-137.6 \pm 7.2$	$-172.9 \pm 21.5^{\text{ns}}$	n.d.
	<i>atakt1</i>		$-139.2 \pm 3.5$	$-192.4 \pm 8.3^{**}$	n.d.
	<i>athak5</i>		$-106.1 \pm 8.6$	$-156.6 \pm 22.2^{\text{ns}}$	n.d.
	<i>athak5 atakt1</i>		$-258.0 \pm 22.9$	$-265.3 \pm 20.8^{\text{ns}}$	n.d.

1 h before leveling off at approximately  $10 \mu\text{mol g}$  (root fresh weight) $^{-1} \text{h}^{-1}$  by the end of the 24-h period.

Despite variations in the sustainability of AWE (Fig. 6),  $\text{NH}_4^+$  withdrawal consistently resulted in increased tissue (shoot, root, and total)  $\text{K}^+$  accumulation over 24 h at all  $\text{K}^+$  levels tested. By the end of 24 h,  $\text{NH}_4^+$  withdrawal resulted in 136%, 150%, and 27% increases in total tissue  $\text{K}^+$  levels under low-, intermediate-, and high- $\text{K}^+$  conditions, respectively (Fig. 7). Interestingly,  $\text{NH}_4^+$  withdrawal over 24 h also resulted in increased tissue accumulation of  $\text{Na}^+$  (Supplemental Fig. S1).

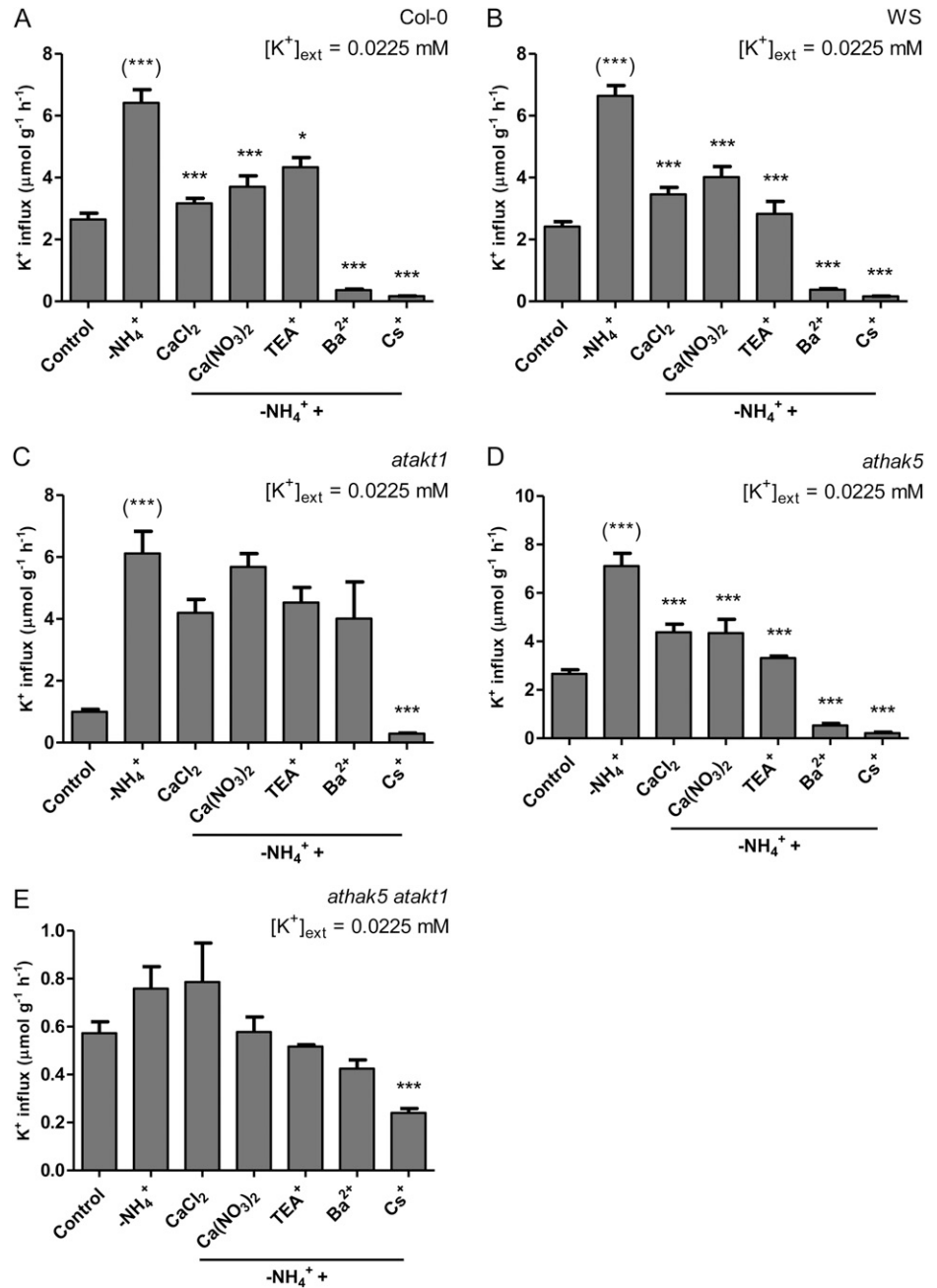
## DISCUSSION

Although the genetic identities of  $\text{K}^+$  channels and high-affinity transporters, and their contributions to high- and low-affinity  $\text{K}^+$  uptake, have been examined extensively in *Arabidopsis*, few studies have placed these fundamental discoveries into the context of agriculturally important species such as barley. In this work, both barley and *Arabidopsis* were grown at high external ammonium concentration ( $[\text{NH}_4^+]_{\text{ext}}$  of 10 and 2 mM, respectively; the difference is a reflection of each species' unique sensitivity to  $\text{NH}_4^+$ ; Britto and Kronzucker, 2002; ten Hoopen et al., 2010) to inhibit high-affinity transporters and thereby isolate  $\text{K}^+$  channel functioning (Hirsch et al., 1998; Spalding et al., 1999; Santa-Maria et al., 2000). We should also note that each species was grown for different lengths of time in different media (see "Materials and Methods"), reflecting their different developmental programs and nutritional preferences. Although differences in growth regime and developmental stage are important to consider, both species displayed severely reduced high-affinity  $\text{K}^+$  uptake due to  $\text{NH}_4^+$  (see below), and this set the stage for critical evaluations and comparisons of  $\text{K}^+$  transporter functioning. At the lowest  $[\text{K}^+]_{\text{ext}}$  tested (0.0225 mM), fundamental differences

in the apparent mechanisms of steady-state  $\text{K}^+$  uptake were observed between the two species (Fig. 8). In both the wild type and *athak5* mutants of *Arabidopsis*,  $\text{K}^+$  influx was blocked by the classic channel inhibitors  $\text{TEA}^+$  and  $\text{Ba}^{2+}$  (Fig. 2, A, B, and D), indicating the involvement of the Shaker-like  $\text{K}^+$  channel AtAKT1 at very low  $[\text{K}^+]_{\text{ext}}$  in this species (and confirming the results of Hirsch et al. [1998] and Spalding et al. [1999]). Moreover, the AtAKT1 knockout lines *atakt1* and *athak5 atakt1* showed significantly lower (59% and 78%) influx than their respective wild types. By contrast, in barley, neither  $\text{TEA}^+$  nor  $\text{Ba}^{2+}$  affected  $\text{K}^+$  influx at this  $[\text{K}^+]_{\text{ext}}$  (Fig. 1A), indicating that it does not appear to involve ( $\text{TEA}^+$ - or  $\text{Ba}^{2+}$ -sensitive) channels; this is consistent with our thermodynamic (Nernstian) analysis based on compartmental and electrophysiological data, which predicted influx to be an active process (Table I). Consistent with this analysis, influx in barley was significantly suppressed by the  $\text{K}^+$  transporter inhibitor  $\text{Cs}^+$ , the metabolic inhibitors  $\text{VO}_4^{3-}$ , DES,  $\text{CN}^- + \text{SHAM}$ , and CCCP, and pH 9.2 (which collapses the electrochemical potential difference for protons). Thus, it appears that steady-state potassium influx at low  $\text{K}^+$  and high  $\text{NH}_4^+$ , while reduced, is mediated by high-affinity transporters in this species, most likely including HvHAK1 (Santa-María et al., 1997). We should note, however, that pH 9.2 also inhibited steady-state influx in *athak5* (Fig. 2D), indicating the possibility of alkalinity-induced AtAKT1 inhibition (Fuchs et al., 2005).

Interestingly, the  $\text{Cs}^+$  sensitivity of  $\text{K}^+$  influx in *athak5 atakt1* double mutants at low  $\text{K}^+$  suggests that a genetically unidentified uptake system is operative, albeit at a relatively minor capacity. This is in contrast to other reports suggesting that "unknown systems" only operate at high  $[\text{K}^+]_{\text{ext}}$  (more than 0.5 mM; Pyo et al., 2010; Rubio et al., 2010). Thus, at least two distinct unknown systems appear to operate in *Arabidopsis*; moreover, the pharmacological profile of *athak5 atakt1* in our study did not

**Figure 5.** The effects of various pharmacological and nutritional treatments on  $K^+$  influx stimulated due to  $NH_4^+$  withdrawal in intact roots of Arabidopsis Col-0 wild type (A), WS wild type (B), *atakt1* (C), *athak5* (D), and *athak5 atakt1* (E) grown in full nutrient medium at low  $[K^+]_{ext}$  and 2 mM  $[NH_4^+]_{ext}$ . Fluxes are indicated on a root fresh weight basis. Asterisks denote different levels of significance between  $-NH_4^+$  and treatment pairs (\* $0.01 < P < 0.05$ , \*\* $0.001 < P < 0.01$ , \*\*\* $P < 0.001$ ; one-way ANOVA with Dunnett's multiple comparison post hoc test). Asterisks in parentheses denote levels of significance between control and  $-NH_4^+$  pairs (Student's *t* test). Each treatment represents the mean of four to 14 replicates. Error bars indicate SE.



match that of others, particularly with respect to  $Ca^{2+}$  and  $Ba^{2+}$  sensitivity (Caballero et al., 2012). This raises the question of whether similar mechanisms are at play in barley at low- $K^+$ , high- $NH_4^+$  conditions and provides avenues for future research.

At  $[K^+]_{ext}$  above 0.1 mM, by contrast,  $K^+$  channels do appear to participate in  $K^+$  uptake in barley, since, at the intermediate  $[K^+]_{ext}$  tested (0.1125 mM), we observed significant inhibition of  $K^+$  influx by TEA $^+$  and  $Ba^{2+}$  (Fig. 1C). Although thermodynamic analyses suggested  $K^+$  uptake at intermediate  $K^+$  to be an active process (Table I), this apparent contradiction most likely reflects some methodological discrepancies. Pharmacological testing

of  $K^+$  influx and compartmental analysis of  $^{42}K^+$  efflux take the entire root into account and thus reflect an average of different cell types along the root axis. On the other hand, electrophysiological measurements of  $\Delta\Psi_m$  are, by nature, single-cell measurements and thus do not necessarily represent the whole root. In fact, membrane polarization is known to follow the longitudinal axis of the root, with the most polarized cells located near the root tip (Hirsch et al., 1998). As our  $\Delta\Psi_m$  measurements were made 2 to 3 cm from the root tip (see "Materials and Methods"), it is likely that we measured from cells not polarized enough to conduct passive  $K^+$  uptake. Thus, at intermediate  $[K^+]_{ext}$  what we observe

may be a mixed population of cells: some conducting channel-mediated  $K^+$  uptake, others engaging high-affinity transporters. At 5 mM  $[K^+]_{ext}$ , where channel-mediated  $K^+$  uptake is proposed to dominate and high-affinity transporters are assumed to be largely irrelevant (Maathuis and Sanders, 1996; Rubio et al., 2010), we did indeed find  $TEA^+$  sensitivity; however, oddly, we also observed stimulations in steady-state  $K^+$  influx with  $BaCl_2$  application (Fig. 1E). Similarly, applications of  $CaCl_2$  and  $Ca(NO_3)_2$  also stimulated  $K^+$  influx (Fig. 1F), while they produced no effect at low and intermediate  $[K^+]_{ext}$  (Fig. 1, B and D, respectively). This may be the result of anion effects specific to the LATS, as demonstrated in earlier reports (Epstein et al., 1963; Kochian et al., 1985). Kochian et al. (1985) showed that  $Cl^-$  stimulated low-affinity  $K^+$  uptake (possibly via coupled transport), unlike  $SO_4^{2-}$ ,  $H_2PO_4^-$ , and (in contrast to this study)  $NO_3^-$ . The apparent contradiction with respect to  $NO_3^-$  could be attributed to a variety of differences in experimental procedures, including species, growth medium, and influx protocol. Surprisingly, further elucidation of the mechanism underlying this effect has not occurred since then; however, this falls out of the scope of our study. What is important to note is that three distinct uptake scenarios appear to occur in barley roots grown under high  $NH_4^+$  and varying  $[K^+]_{ext}$ : at low  $K^+$ , an active process dominates, attributable to residual HvHAK1 activity and/or unknown systems; at intermediate  $K^+$ , a mixed population of channel (HvAKT1)- and high-affinity transporter (HvHAK1)-mediated  $K^+$  uptake occurs; and at high  $K^+$ , channel (HvAKT1)-mediated  $K^+$  uptake appears to dominate, but with unique  $Cl^-$ - and  $NO_3^-$ -induced stimulations (Fig. 8).

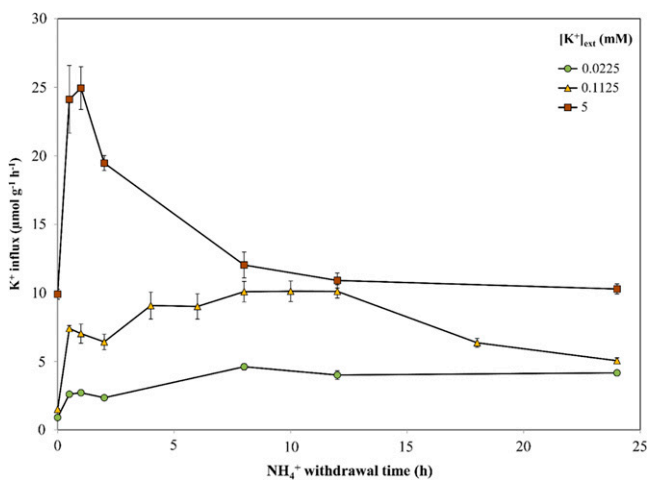


**Figure 6.** Responses of  $K^+$  influx to the duration of  $NH_4^+$  withdrawal in roots of intact barley seedlings grown under full nutrient medium, various  $[K^+]_{ext}$  levels, and 10 mM  $[NH_4^+]_{ext}$ . Fluxes are indicated on a root fresh weight basis. Each data point represents the mean of four replicates. Error bars indicate SE. [See online article for color version of this figure.]

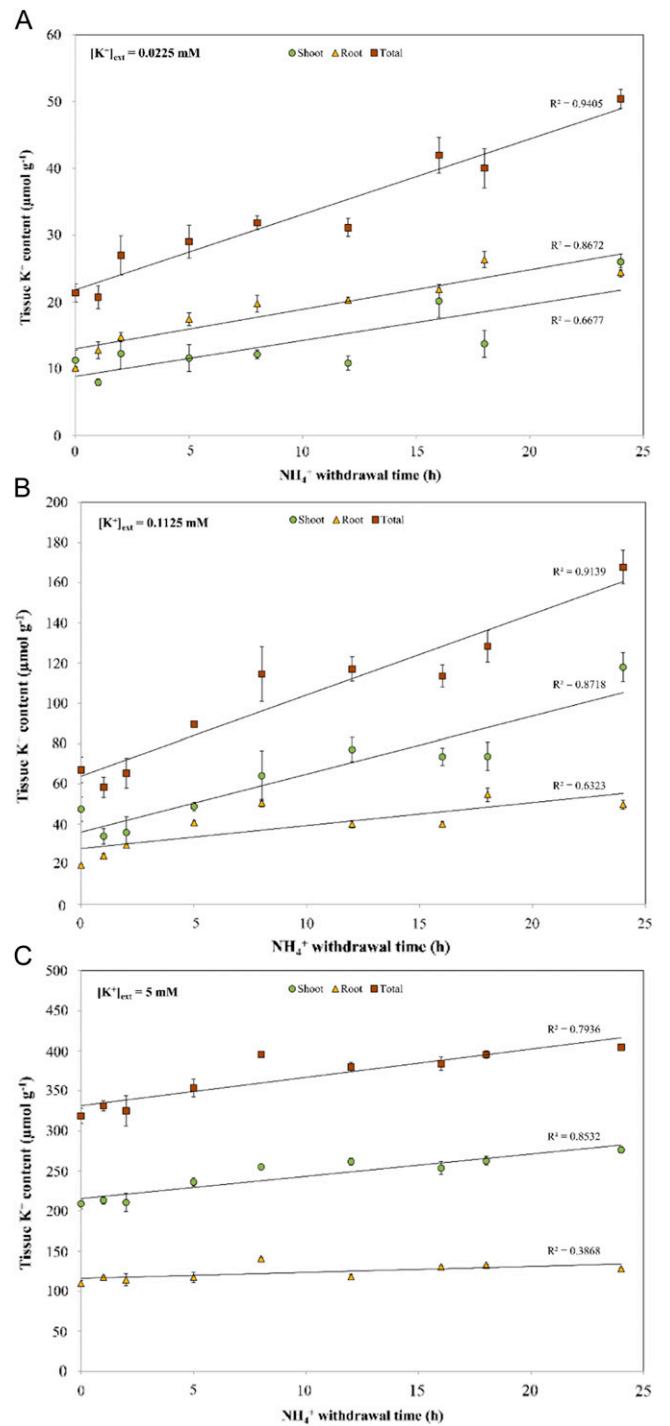


**Figure 7.** Responses of tissue  $K^+$  content to the duration of  $NH_4^+$  withdrawal in barley seedlings grown under full nutrient medium at low (A), intermediate (B), and high (C)  $[K^+]_{ext}$  and 10 mM  $[NH_4^+]_{ext}$ . Content measurements are indicated on a root fresh weight basis. Each data point represents the mean of four replicates. Error bars indicate SE. [See online article for color version of this figure.]

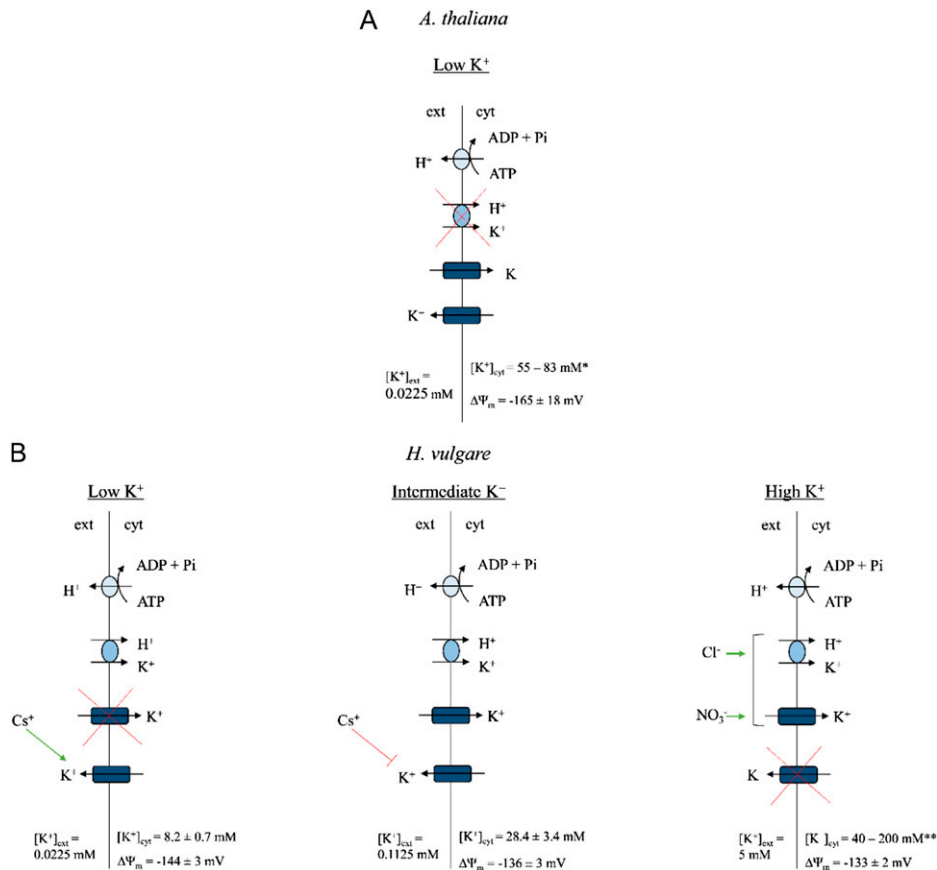


**Figure 8.** Schematic overview of  $K^+$  uptake in plant roots under steady-state conditions (i.e. in the presence of high [millimolar]  $[NH_4^+]_{ext}$ ). Under low (0.0225 mM)  $[K^+]_{ext}$ ,  $K^+$  uptake is predominantly mediated by  $K^+$  channels (AtAKT1) in Arabidopsis (Col-0 wild type; A), whereas in barley (B),  $K^+$  channels do not operate and uptake is likely mediated by high-affinity transporters (HvHAK1), albeit at a residual capacity due to  $NH_4^+$ -induced inhibition. Above intermediate  $K^+$  levels ( $[K^+]_{ext} = 0.1125 \text{ mM}$ ),  $K^+$  channels do operate in barley, with further  $Cl^-$ - and  $NO_3^-$ -induced stimulations of  $K^+$  uptake observed at high  $K^+$  ( $[K^+]_{ext} = 5 \text{ mM}$ ). In barley,  $K^+$  efflux is likely channel mediated at low and intermediate  $K^+$ , although with varying sensitivities to  $Cs^+$ , whereas  $K^+$  efflux is likely inoperative at high  $K^+$ .  $K^+$  efflux in Arabidopsis is also likely channel mediated (Maathuis and Sanders, 1993).  $[K^+]_{cyt}$  and resting  $\Delta\Psi_m$  values, when measured, are also listed. Asterisks refer to references as follows: \*see Maathuis and Sanders (1993) and Halperin and Lynch (2003); \*\*see Leigh and Wyn-Jones (1984), Walker et al. (1996), and Kronzucker et al. (2006). [See online article for color version of this figure.]

Consistent across all  $[K^+]_{ext}$  tested in barley is the significant reduction of  $K^+$  influx by metabolic inhibitors (Fig. 1, A, C, and E). Typically, the HATS is reported to be more sensitive to metabolic inhibitors compared with the LATS (Malhotra and Glass, 1995); however, the vast majority of metabolic inhibitors was most effective in suppressing influx at the intermediate  $K^+$  level and not at the lowest level. Interestingly, influx at intermediate  $K^+$  was most strongly inhibited by  $Cs^+$  and was the most stimulated in response to  $NH_4^+$  withdrawal. Perhaps this is indicative of the mixed population of channels and high-affinity transporters operating under these conditions and reflects a highly dynamic transport capacity. Also evident is the lack of NSCC involvement at all  $[K^+]_{ext}$  tested, as  $Ca^{2+}$ ,  $Gd^{3+}$ ,  $La^{3+}$ ,  $Glu$ , and DEPC had no effect on  $K^+$  influx (Fig. 1, B, D, and F; Essah et al., 2003). It is rather surprising that, if NSCCs catalyze high rates of cation fluxes, as has been proposed

(White and Davenport, 2002; Essah et al., 2003; Kronzucker and Britto, 2011, and refs. therein), we were unable to observe their activity physiologically. However, the presence of significant concentrations of  $Ca^{2+}$  (1–5 mM), reflective of common soil conditions (Garcia-deblás et al., 2003; Zhang et al., 2010), may have reduced putative  $K^+$  currents through NSCCs considerably (White and Davenport, 2002). Similarly,  $Na^+$ - $K^+$  cotransport does not appear to be operative, as no effect of 10 mM NaCl on  $K^+$  influx was observed (data not shown), ruling out the involvement of HKT/TRK-type transporters (Rubio et al., 1995). It is worth highlighting here that pharmacological profiling, like any experimental method, is not without its caveats. Although a traditionally useful tool for gaining insight into the structure and function of membrane transporters, particularly in planta, the lack of specificity of several blockers/chemical treatments (White and Broadley, 2000; Coskun et al., 2012), as well

as the need to employ relatively high concentrations at times, can potentially have secondary (“pleiotropic”) effects. This by no means invalidates the use of pharmacology but simply speaks to the importance of a multipronged approach in such studies.

As with influx, efflux analysis in barley demonstrates that distinct mechanisms are at play at each of the three  $[K^+]_{ext}$  tested (Fig. 8). At low  $K^+$ , where influx was determined to be solely active, we see the perplexing result of efflux stimulation upon  $Cs^+$  application (Fig. 3A). Testing of the involvement of  $Cs^+$ -induced depolarizations in this phenomenon (Nocito et al., 2002) yielded negative results (data not shown). We should note that instances of cellular  $K^+/Cs^+$  exchange have been documented in the animal literature (Beaugé et al., 1973; Guerin and Wallon, 1979); however, to our knowledge, no precedence exists in the plant literature. Moreover, this does not explain its isolated incidence at low  $[K^+]_{ext}$ ; thus, the mechanism remains unknown. In stark contrast with these observations, both  $Cs^+$  and  $TEA^+$  significantly inhibited  $K^+$  efflux at intermediate  $K^+$  levels (Fig. 3B). This effect has also been observed at a similar  $[K^+]_{ext}$  (0.1 mM) under an  $NO_3^-$  background (Coskun et al., 2010) and is consistent with other reports of the  $Cs^+$  and  $TEA^+$  sensitivities of channel-mediated ion fluxes (Krol and Trebacz, 2000; White and Broadley, 2000). At the highest  $[K^+]_{ext}$  tested (5 mM), a third scenario emerged, one in which physiological efflux was ruled out, as was previously shown under low-affinity conditions with  $NO_3^-$ -grown barley (Coskun et al., 2010). While an examination of the mechanisms of  $K^+$  efflux was beyond the scope of this study, physiological-efflux data at low and intermediate  $[K^+]_{ext}$  lend themselves to compartmental analysis (Lee and Clarkson, 1986; Siddiqi et al., 1991; Kronzucker et al., 1995). In these cases, we have strong evidence that efflux at low and intermediate  $K^+$  is occurring from the cytosol and across the plasma membrane, allowing us to confidently estimate  $[K^+]_{cyt}$  (Table I). The variability of these results also confirms some of the earlier work on barley by Kronzucker et al. (2003), which investigated the heterostasis of  $[K^+]_{cyt}$  in particular its suppression on high- $NH_4^+$  medium. The lack of physiological efflux at high  $K^+$  prevents us from making such estimates. Future studies will examine the differences in  $K^+$  efflux between  $NO_3^-$ - and  $NH_4^+$ -grown plants and may help provide insight into the mechanisms of  $NH_4^+$  toxicity.

Withdrawal of  $NH_4^+$  resulted in immediate and dramatic stimulations of  $K^+$  influx, as high as 4.5-fold in barley and 6-fold in Arabidopsis. We should note that there have been a few reports of  $K^+$  uptake stimulation upon  $NH_4^+$  withdrawal in both barley (Santa-María et al., 2000) and Arabidopsis (Rubio et al., 2010); however, little attention was directed to this phenomenon. In addition, the magnitude of unidirectional fluxes measured was minuscule in one study [approximately  $1 \mu\text{mol g (root fresh weight)}^{-1} \text{h}^{-1}$ ; Santa-María et al., 2000] and not measured in the other (Rubio et al., 2010). By contrast, some of the fluxes recorded in this study at high  $K^+$  in barley [ $25\text{--}36 \mu\text{mol g (root fresh weight)}^{-1} \text{h}^{-1}$ ]

are among the highest bona fide transmembrane fluxes of  $K^+$  reported. Although some published rates of unidirectional  $Na^+$  and  $NH_4^+$  fluxes under toxicity conditions are larger [e.g.  $60\text{--}600 \mu\text{mol g (root fresh weight)}^{-1} \text{h}^{-1}$ ; Lazof and Cheeseman, 1986; Britto et al., 2001; Essah et al., 2003; Horie et al., 2007; Szczerba et al., 2008], these values have come into question, particularly with respect to the improbably high energy costs of such fluxes (Britto and Kronzucker, 2009). In this study, these powerful stimulations of  $K^+$  influx might be explained by the significant hyperpolarizations observed upon  $NH_4^+$  withdrawal (Table II). At low and intermediate  $K^+$  levels, these electrical changes translate into thermodynamic shifts from active to passive  $K^+$  uptake in barley, the latter driven by a powerful downhill gradient; this was confirmed by use of the channel-blocking agents  $TEA^+$ ,  $Ba^{2+}$ , and  $Cs^+$  (Figs. 4 and 5). Interestingly, AWE was observed in both *atakt1* and *athak5* knockout lines (Fig. 5, C and D) and was substantial in both cases (513% and 167% of control values, respectively), suggesting a sizable participation by both transporters. This result demonstrates that AtHAK5 can operate under thermodynamically passive conditions, lending support to the idea that some HAK/KUP/KT transporters have a dual-affinity nature (Fu and Luan, 1998; Kim et al., 1998). However, it is not clear whether it would function under these conditions as an  $H^+/K^+$  symporter (Gierth and Mäser, 2007) or engage a channel-like mechanism (Fu and Luan, 1998). Further experimentation is required to address this possibility. The fact that AWE was minor in *athak5 atakt1* double mutants suggests that AtAKT1 and AtHAK5 are the major contributors, and any contribution from unknown systems is small (Fig. 5E), as it is under steady-state conditions (Fig. 2E). Lastly, the inhibition of  $K^+$  efflux upon  $NH_4^+$  withdrawal at low and intermediate  $K^+$  (Fig. 3, A and B, insets) is further evidence for a shift in thermodynamic gradients; under these conditions, it is likely that physiological  $K^+$  efflux has shut down entirely.

Pharmacological profiling of AWE across all  $[K^+]_{ext}$  clearly implicated channel (AKT1) involvement; however, the response of AWE to external  $Ca^{2+}$  revealed some unusual results. At low and intermediate  $K^+$ , AWE was all but suppressed by  $Ca^{2+}$  in barley (Fig. 4, A and B). This effect was not observed at high  $K^+$ , however:  $CaSO_4$  had no effect, while  $CaCl_2$  and  $Ca(NO_3)_2$  both stimulated AWE, by 26% and 47%, respectively (Fig. 4C). The  $Ca^{2+}$  sensitivity of AWE was also observed in Arabidopsis wild-type lines and *athak5* mutants at low  $K^+$  (Fig. 5, A, B, and D). Surprisingly, it was not observed in AtAKT1 knockout lines (Fig. 5, C and E), suggesting that the  $Ca^{2+}$  sensitivity of AWE is linked to the AtAKT1 channel. To our knowledge, evidence of AtAKT1 blockage by external  $Ca^{2+}$  is sparse; in one case, though, a weak inhibition of inward-rectifying  $K^+$  channels in the plasma membrane of rye roots by high concentrations of  $Ca^{2+}$  was observed (White and Lemtiri-Chlieh, 1995), which provides evidence that  $K^+$  channels, such as AtAKT1, may be sensitive to extracellular  $Ca^{2+}$  under some conditions. An alternative hypothesis, that  $Ca^{2+}$  coprovision

coincides with an increased  $\text{Ca}^{2+}$  influx, resulting in less hyperpolarization and thus a reduced  $\text{K}^+$  flux, was ruled out in two ways. First, the  $\text{Ca}^{2+}$  channel inhibitor verapamil (Lee and Tsien, 1983; compare with White, 1998) was supplied alongside  $\text{Ca}^{2+}$  during  $\text{NH}_4^+$  withdrawal, with no effects observed (data not shown). Second, when  $\Delta\Psi_m$  was measured during  $\text{Ca}(\text{NO}_3)_2$  coprovision with  $\text{NH}_4^+$  withdrawal, not only was the hyperpolarization undiminished, but, in fact, even greater hyperpolarization was measured (Table II). Surprisingly, however, at high  $\text{K}^+$ , membrane hyperpolarization was reduced, even though  $\text{Ca}(\text{NO}_3)_2$  provision upon  $\text{NH}_4^+$  withdrawal resulted in even greater  $\text{K}^+$  influx than  $\text{NH}_4^+$  withdrawal alone (Table II). Thus, it appears that AWE and its stimulation or inhibition do not solely depend on membrane polarization but involve other processes, such as channel gating (as with  $\text{Ca}^{2+}$  effects) or coupling to anion transport (as in the case of  $\text{Cl}^-$  and  $\text{NO}_3^-$  effects). This is further confirmed by the fact that the greatest AWE occurred in barley at intermediate  $\text{K}^+$  (355% increase from control) while the concomitant hyperpolarizations were no greater than that seen at other  $\text{K}^+$  levels (Table II). Also, the largest relative AWE in Arabidopsis was seen in *atakt1* (513%), but it, too, showed hyperpolarization no greater than in any other line (Table II).

A 24-h time course revealed the upper limits of AWE on  $\text{K}^+$  influx, both in terms of magnitude and sustainability. At high  $\text{K}^+$ , influx peaked at approximately  $25 \mu\text{mol g (root fresh weight)}^{-1} \text{h}^{-1}$  by 1 h, in contrast with low and intermediate  $\text{K}^+$ , at which the fluxes continued to rise over 24 and 8 h, respectively (Fig. 6). Nevertheless, all time courses resulted in increased accumulation of tissue  $\text{K}^+$ , demonstrating the nutritional significance of this effect (Fig. 7). Interestingly, at low and intermediate  $\text{K}^+$ ,  $\text{NH}_4^+$  withdrawal also resulted in significant tissue accumulation of  $\text{Na}^+$  (Supplemental Fig. S1), particularly in the roots. This may reflect the ability of  $\text{Na}^+$  to replace  $\text{K}^+$  in some of its cellular roles (Subbarao et al., 2003), since these growth conditions (low and intermediate  $[\text{K}^+]_{\text{ext}}$ , high  $[\text{NH}_4^+]_{\text{ext}}$ ) are toxic for barley and result in extremely low tissue  $\text{K}^+$  levels (Fig. 7). Some reports suggest that  $\text{Na}^+$  and  $\text{K}^+$  could share similar uptake mechanisms, such as  $\text{K}^+$  channels (for review, see Kronzucker and Britto, 2011); thus, situations where stimulated channel activity is induced could account for these findings. While out of the scope of this work, it would be interesting to measure  $\text{Na}^+$  fluxes in such a scenario, especially in the toxic range, to better understand the mechanisms of  $\text{Na}^+$  transport.

We have demonstrated here that the Arabidopsis model of  $\text{K}^+$  acquisition is not universally applicable. Although  $\text{K}^+$  channels appear to be the sole means of  $\text{K}^+$  acquisition under low- $\text{K}^+$ , high- $\text{NH}_4^+$  conditions in Arabidopsis, this is not the case for barley. Our study provides new physiological evidence of three distinct modes of  $\text{K}^+$  influx and efflux in  $\text{NH}_4^+$ -grown barley, operating at 0.0225, 0.1125, and 5 mM  $[\text{K}^+]_{\text{ext}}$ . Figure 8 illustrates these key findings. Moreover, we demonstrate that  $\text{NH}_4^+$  withdrawal can reveal a very high capacity and plasticity among  $\text{K}^+$  transporters. This work provides a framework

of characteristics, including nutritional and pharmacological profiles, by which discoveries in molecular genetics, particularly in the emerging field of cereal genomics, can be gauged.

## MATERIALS AND METHODS

### Plant Culture

Seeds of barley (*Hordeum vulgare* 'Metcalfe') were surface sterilized for 15 min in 1% sodium hypochlorite and germinated under acid-washed sand for 3 d prior to placement in 14-L vessels containing aerated modified Johnson's nutrient solution. All solutions were composed of 5 mM  $(\text{NH}_4)_2\text{SO}_4$ , 0.5 mM  $\text{NaH}_2\text{PO}_4$ , 0.25 mM  $\text{MgSO}_4$ , 0.2 mM  $\text{CaSO}_4$ , 25  $\mu\text{M}$   $\text{H}_3\text{BO}_3$ , 20  $\mu\text{M}$  FeEDTA, 6.25  $\mu\text{M}$   $\text{CaCl}_2$ , 2  $\mu\text{M}$   $\text{ZnSO}_4$ , 0.5  $\mu\text{M}$   $\text{MnSO}_4$ , 0.5  $\mu\text{M}$   $\text{CuSO}_4$ , and 0.125  $\mu\text{M}$   $\text{Na}_2\text{MoO}_4$  (pH adjusted to 6.2–6.3, using 1 M NaOH).  $\text{K}^+$  was supplied at 0.0225 (low), 0.1125 (intermediate), or 5 mM (high) as  $\text{K}_2\text{SO}_4$ . Solutions were completely exchanged on days 5 (for all  $\text{K}^+$  conditions) and 6 (for low- and intermediate- $\text{K}^+$  conditions) following germination to ensure that plants remained at a nutritional steady state for experimentation on day 7. Plants were grown in a climate-controlled, walk-in growth chamber under fluorescent lights, with an irradiation of 200  $\mu\text{mol photons m}^{-2} \text{s}^{-1}$  at plant height, for 16 h  $\text{d}^{-1}$  (Philips Silhouette High Output F54T5/850HO; Philips Electronics). Daytime temperature was 20°C, nighttime temperature was 15°C, and relative humidity was approximately 70%.

Seeds of Arabidopsis (*Arabidopsis thaliana*) wild-type ecotypes Col-0 (N1092) and WS (N1601) and transfer DNA insertion lines *atakt1-1* (CS3762; WS ecotype), *athak5-1* (SALK\_014177; Col-0 ecotype), and *athak5 atakt1* (Col-0 ecotype; Rubio et al., 2010) were surface sterilized for 5 min with 70% ethanol, followed by 10 min with a 1% sodium hypochlorite-0.05% SDS mixture, and allowed to stratify in a 0.1% agar solution in the dark for 3 d at 4°C, prior to germination on acid-washed sand for 4 d. Seedlings were placed in 14-L vessels containing aerated nutrient solution composed of 5 mM  $\text{K}_2\text{SO}_4$ , 1 mM  $\text{Ca}(\text{NO}_3)_2$ , 1 mM  $\text{NaH}_2\text{PO}_4$ , 0.5 mM  $\text{MgSO}_4$ , 0.25 mM  $\text{CaSO}_4$ , 25  $\mu\text{M}$   $\text{H}_3\text{BO}_3$ , 20  $\mu\text{M}$  FeEDTA, 2  $\mu\text{M}$   $\text{ZnSO}_4$ , 0.5  $\mu\text{M}$   $\text{MnCl}_2$ , 0.5  $\mu\text{M}$   $\text{CuSO}_4$ , and 0.5  $\mu\text{M}$   $\text{Na}_2\text{MoO}_4$  (pH 6.0, with 1 M NaOH). Solutions were completely exchanged once per week for 3 weeks. During the final (5th) week of growth,  $[\text{K}^+]_{\text{ext}}$  was reduced to 0.0225 mM and  $\text{Ca}(\text{NO}_3)_2$  was replaced with an equimolar (1 mM) amount of  $(\text{NH}_4)_2\text{SO}_4$ . Nutrient solutions were completely exchanged every other day during the final week of growth and experimented with on day 35. Such a growth regime was particularly important for the proper growth of *atakt1* and *athak5 atakt1* mutants, as germination and growth were severely hindered on low- $\text{K}^+$ , high- $\text{NH}_4^+$  medium (data not shown; Rubio et al., 2010). Plants were grown in a climate-controlled chamber under fluorescent lights, with an irradiation of 200  $\mu\text{mol photons m}^{-2} \text{s}^{-1}$  at plant height, for 12 h  $\text{d}^{-1}$  (Philips F96T8/TL841/HO/PLUS; Philips Electronics). Daytime temperature was 20°C, nighttime temperature was 15°C, and relative humidity was approximately 70%.

### Direct Influx

Unidirectional  $\text{K}^+$  influx in roots of intact barley and Arabidopsis was measured as described in detail elsewhere (Coskun et al., 2010). In brief, roots of replicate units of three to four plants were preequilibrated for 5 or 10 min (see below) in a solution either identical to the growth solution (control) or in growth solution supplemented with a chemical treatment (see below). Roots were then immersed for 5 min in a solution identical to the preequilibration solution but containing  $^{42}\text{K}$  (half-life = 12.36 h), received as  $^{42}\text{K}_2\text{CO}_3$  from the McMaster University Nuclear Reactor. Labeled plants were transferred to nonradioactive growth solution for 5 s to reduce tracer carryover and further desorbed of radioactivity from the extracellular space for 5 min in fresh growth solution. Based on the half-times of cytosolic exchange and efflux-influx ratios reported in Table I,  $\text{K}^+$  influx was underestimated by no more than 5% due to efflux during desorption (Britto and Kronzucker, 2001). Immediately following desorption, roots were detached from shoots and spun in a low-speed centrifuge for 30 s to remove surface solution prior to weighing. Radioactivity in root tissues was counted (shoot counts were not detectable) and corrected for isotopic decay using one of two  $\gamma$  counters (Perkin-Elmer Wallac 1480 Wizard 3' and Packard Instrument Quantum Cobra Series II, model 5003). Throughout,  $\text{K}^+$  influx is expressed in terms of  $\mu\text{mol g (root fresh weight)}^{-1} \text{h}^{-1}$ .

## Compartmental Analysis by Tracer Efflux

$^{42}\text{K}^+$  efflux from roots on intact barley was examined as described previously (Coskun et al., 2010) and based on the method of compartmental analysis (Lee and Clarkson, 1986; Siddiqi et al., 1991; Kronzucker et al., 1995). In brief, roots of replicate units of five to 10 seedlings were immersed for 1 h in aerated nutrient medium identical to growth conditions but containing  $^{42}\text{K}$  (see above). Labeled seedlings were secured in glass efflux funnels, and roots were eluted of radioactivity with successive 20-mL aliquots of aerated, non-radioactive growth solution. The desorption series was timed as follows, from first to final eluate: 15 s (four times), 20 s (three times), 30 s (two times), 40 s (once), 50 s (once), 1 min (five times), 1.25 min (once), 1.5 min (once), 1.75 min (once), 2 min (13 times), for a total of 40 min of elution. The first 19 eluates (14 min into the elution series) were identical to the growth solution, and the final 13 eluates contained either growth solution (control) or a chemical treatment (see below).

Immediately following elution, plant organs were harvested as described in the preceding section, and radioactivity from eluates, roots, and shoots was counted and corrected for isotopic decay, as described above. For comparison charts of  $^{42}\text{K}$  efflux, the specific activities of all replicates were normalized to the arbitrary value of  $2 \times 10^5$  cpm  $\mu\text{mol}^{-1}$ . Throughout,  $^{42}\text{K}^+$  efflux is expressed in terms of cpm released g (root fresh weight) $^{-1}$  min $^{-1}$ .

For the results in Table I, tracer efflux and retention data were used to estimate unidirectional and net fluxes, and cytosolic half-times of exchange and pool sizes, according to the methods of compartmental analysis (Kronzucker et al., 1995). In brief, linear regression of the function  $\ln \Phi_{\text{co}(i)}^* = \ln \Phi_{\text{co}(i)}^* - kt$  [where  $\Phi_{\text{co}(i)}^*$  is tracer efflux at elution time  $t$ ,  $\Phi_{\text{co}(i)}^*$  is initial tracer efflux, and  $k$  is the rate constant describing the exponential decline in radioactive tracer efflux, found from the slope of the tracer release rate; Fig. 3] was used to resolve the kinetics of the slowest exchanging (cytosolic) phase in these experiments (Kronzucker et al., 1995). The cytosolic origin of the slowest exchanging phase was confirmed for the low- and intermediate- $\text{K}^+$  conditions, and ruled out for the high- $\text{K}^+$  condition, by means of pharmacological testing (Fig. 3; Coskun et al., 2010); thus, compartmental analysis could not be performed at high  $\text{K}^+$ . Based on literature precedents demonstrating the relatively long half-times of vacuolar  $\text{K}^+$  exchange compared with that of the cytosol (hours versus minutes; Poole, 1971; Walker and Pitman, 1976; Behl and Jeschke, 1982; Memon et al., 1985; Hajibagheri et al., 1988; Siddiqi et al., 1991; White et al., 1991), we could assume that the vast majority of intracellular tracer released was from the cytosolic pool after only 1 h of loading. Chemical efflux,  $\Phi_{\text{cor}}$ , was determined from  $\Phi_{\text{co}(i)}^*$ , divided by the specific activity of the cytosol ( $\text{SA}_{\text{cyt}}$ ) at the end of the labeling period.  $\text{SA}_{\text{cyt}}$  was estimated by using external specific activity ( $\text{SA}_{\text{ext}}$ ), labeling time  $t$ , and the rate constant  $k$ , which are related in the exponential rise function  $\text{SA}_{\text{cyt}} = \text{SA}_{\text{ext}}(1 - e^{-kt})$  (Walker and Pitman, 1976). Net flux,  $\Phi_{\text{net}}$ , was found using total plant (root and shoot)  $^{42}\text{K}$  retention after desorption, and influx,  $\Phi_{\text{ac}}$ , was calculated from the sum of  $\Phi_{\text{co}}$  and  $\Phi_{\text{net}}$ . Note that shoot accumulation of radiotracer is routinely dealt with in compartmental analysis of intact seedlings (Jeschke and Jambor, 1981; Siddiqi et al., 1991); thus, the parameters listed in Table I can be accurately estimated.  $[\text{K}^+]_{\text{cyt}}$  was determined using the flux turnover equation,  $[\text{K}^+]_{\text{cyt}} = \Omega \Phi_{\text{ac}} k^{-1}$ , where  $\Omega$  is a proportionality constant correcting for cytosolic volume being approximately 5% of total tissue (Lee and Clarkson, 1986; Siddiqi et al., 1991).

## Pharmacological/Chemical Treatments

For  $\text{K}^+$  influx experiments, the following agents were used to test for the involvement of different uptake mechanisms: 10 mM TEACl, 5 mM  $\text{BaCl}_2$ , 10 mM CsCl, 10 mM  $\text{Na}_3\text{VO}_4$ , 100  $\mu\text{M}$  DNP (1% ethanol), 50  $\mu\text{M}$  DES (1% ethanol), 1 mM NaCN + SHAM, 10  $\mu\text{M}$  CCCP (1% ethanol), pH 9.2 (adjusted with 1 M NaOH), 5 mM  $\text{CaSO}_4$ , 5 mM  $\text{CaCl}_2$  (1 mM in the case of Arabidopsis; see "Results"), 5 mM  $\text{Ca}(\text{NO}_3)_2$  (1 mM for Arabidopsis), 50  $\mu\text{M}$   $\text{GdCl}_3$ , 50  $\mu\text{M}$   $\text{LaCl}_3$ , 10 mM sodium Glu, and 100  $\mu\text{M}$  DEPC. All treatments involved a 5-min pretreatment, except for DNP, DES,  $\text{CN}^-$  + SHAM, CCCP, and DEPC, which took 10 min. It should be noted that no effect of 1% ethanol (a vehicle for DNP, DES, and CCCP) on  $\text{K}^+$  influx was found (data not shown). Inhibitors were added in the presence of a complete growth medium, including  $\text{NH}_4^+$ , except when it was withdrawn for AWE experiments (see "Results").

For  $\text{K}^+$  efflux experiments, eluates were supplemented with 10 mM CsCl, 10 mM TEACl, 5 mM  $\text{BaCl}_2$ , or 5 mM  $\text{CaSO}_4$ . Other treatments involved growth solution without  $(\text{NH}_4)_2\text{SO}_4$ . A small subset of experiments also involved the loading and elution solutions altered to pH 9.2 (with 1 M NaOH).

## Electrophysiology

Measurements of  $\Delta\Psi_m$  from epidermal and cortical root cells of barley and Arabidopsis (aged 7–8 d and 35–37 d, respectively) were conducted as described previously (Schulze et al., 2012). In brief, roots were immersed in a Plexiglas chamber filled with nutrient solution and installed onto the stage of an inverted light microscope (Leica DME; Leica Microsystems). Microelectrodes (tip diameter  $< 1 \mu\text{m}$ ), made from borosilicate glass (i.d. = 0.75 mm, o.d. = 1.00 mm; World Precision Instruments) and produced using an electrode puller (P-30; Sutter Instrument), were filled with 3 M KCl solution (pH 2). Both impaling and reference electrodes were prepared in this manner.  $\Delta\Psi_m$  measurements were made in a region 2 to 3 cm from the root tip, with the use of an electrometer (Duo 773; World Precision Instruments), and recorded on an oscilloscope (TDS2002B; Tektronix). Once steady readings were obtained, treatment solution was perfused through Tygon tubing via a peristaltic pump at a rate of approximately  $7.5 \text{ mL min}^{-1}$ . Treatments included growth solution with  $(\text{NH}_4)_2\text{SO}_4$  excluded with or without an equimolar amount of  $\text{Ca}(\text{NO}_3)_2$ .

Table I displays the results of a thermodynamic (Nernstian) analysis.  $E_{\text{K}^+}$  was estimated using the Nernst equation:

$$E_{\text{K}^+} = \frac{RT}{zF} \ln \frac{[\text{K}^+]_{\text{ext}}}{[\text{K}^+]_{\text{cyt}}}$$

where  $R$  is the universal gas constant ( $8.314 \text{ J K}^{-1} \text{ mol}^{-1}$ ),  $T$  is ambient temperature (293.15 K),  $z$  is the ionic charge of the species (+1 for  $\text{K}^+$ ),  $F$  is the Faraday constant ( $96,485 \text{ C mol}^{-1}$ ), and  $[\text{K}^+]_{\text{ext}}$  and  $[\text{K}^+]_{\text{cyt}}$  are as defined previously (for activity coefficients, see "Results").

## Tissue Content

Tissue  $\text{K}^+$  and  $\text{Na}^+$  contents for barley (aged 7 d) were determined by methods described previously for steady-state and non-steady-state conditions (Britto et al., 2010; Coskun et al., 2012). In brief, replicate units of three to five seedlings had their roots incubated for 5 min in 10 mM  $\text{CaSO}_4$  to release extracellular  $\text{K}^+/\text{Na}^+$  (steady state) or were treated in growth solution with  $\text{NH}_4^+$  removed for various time points spanning 24 h (see "Results"; non steady state) prior to  $\text{CaSO}_4$  desorption. From there, plant organs were harvested as above (see "Direct Influx"), oven dried for 3 d at  $80^\circ\text{C}$  to  $90^\circ\text{C}$ , and pulverized and digested in 30%  $\text{HNO}_3$  for an additional 3 d.  $\text{K}^+$  and  $\text{Na}^+$  concentrations of tissue digests were measured using a dual-channel flame photometer (model 2655-10; Cole-Parmer Instrument). Tissue ion concentration is expressed in  $\mu\text{mol g}$  (root fresh weight) $^{-1}$ .

## Statistics

For influx experiments, each treatment was replicated a minimum of four times and tested for statistical significance with the use of a one-way ANOVA with Dunnett's multiple comparison post hoc test (with steady-state or  $\text{NH}_4^+$  withdrawal-induced flux as a control; see "Results"). For efflux analyses, each treatment was replicated a minimum of three times. Significance testing of each treatment was conducted by matching each pair of data points for a given elution time between treatment and control traces and running Student's  $t$  test (Coskun et al., 2010). The percentages of paired points that were found to be significantly different ( $P < 0.05$ ) are shown in Figure 3 (Coskun et al., 2010).

## Supplemental Data

The following materials are available in the online version of this article.

**Supplemental Figure S1.** Response of tissue  $\text{Na}^+$  content to duration of  $\text{NH}_4^+$  withdrawal in barley seedlings grown under full nutrient medium at low, intermediate, and high  $[\text{K}^+]_{\text{ext}}$  and 10 mM  $[\text{NH}_4^+]_{\text{ext}}$ .

## ACKNOWLEDGMENTS

We thank R. Pasuta and M. Butler (McMaster University Nuclear Reactor) for the provision of  $^{42}\text{K}$ , F. Rubio (Centro de Edafología y Biología Aplicada del Segura-Consejo Superior de Investigaciones Científicas) for his kind donation of *athak5 atakt1* seed material, and A. Walsh (University of Toronto) for his assistance with experimentation.

Received February 6, 2013; accepted March 31, 2013; published April 3, 2013.

## LITERATURE CITED

- Ahn SJ, Shin R, Schachtman DP (2004) Expression of *KT/KLIP* genes in Arabidopsis and the role of root hairs in K<sup>+</sup> uptake. *Plant Physiol* **134**: 1135–1145
- Alemán F, Nieves-Cordones M, Martínez V, Rubio F (2011) Root K<sup>(+)</sup> acquisition in plants: the Arabidopsis thaliana model. *Plant Cell Physiol* **52**: 1603–1612
- Amrutha RN, Sekhar PN, Varshney RK, Kishor PBK (2007) Genome-wide analysis and identification of genes related to potassium transporter families in rice (*Oryza sativa* L.). *Plant Sci* **172**: 708–721
- Ashley MK, Grant M, Grabov A (2006) Plant responses to potassium deficiencies: a role for potassium transport proteins. *J Exp Bot* **57**: 425–436
- Beaugé LA, Medici A, Sjödin RA (1973) The influence of external caesium ions on potassium efflux in frog skeletal muscle. *J Physiol* **228**: 1–11
- Behl R, Jeschke WD (1982) Potassium fluxes in excised barley roots. *J Exp Bot* **33**: 584–600
- Bertl A, Reid JD, Sentenac H, Slayman CL (1997) Functional comparison of plant inward-rectifier channels expressed in yeast. *J Exp Bot (Spec No)* **48**: 405–413
- Brenchley R, Spannagl M, Pfeifer M, Barker GLA, D'Amore R, Allen AM, McKenzie N, Kramer M, Kerhornou A, Bolser D, et al (2012) Analysis of the bread wheat genome using whole-genome shotgun sequencing. *Nature* **491**: 705–710
- Britto DT, Ebrahimi-Ardebili S, Hamam AM, Coskun D, Kronzucker HJ (2010) <sup>42</sup>K analysis of sodium-induced potassium efflux in barley: mechanism and relevance to salt tolerance. *New Phytol* **186**: 373–384
- Britto DT, Kronzucker HJ (2001) Can unidirectional influx be measured in higher plants? A mathematical approach using parameters from efflux analysis. *New Phytol* **150**: 37–47
- Britto DT, Kronzucker HJ (2002) NH<sub>4</sub><sup>+</sup> toxicity in higher plants: a critical review. *J Plant Physiol* **159**: 567–584
- Britto DT, Kronzucker HJ (2008) Cellular mechanisms of potassium transport in plants. *Physiol Plant* **133**: 637–650
- Britto DT, Kronzucker HJ (2009) Ussing's conundrum and the search for transport mechanisms in plants. *New Phytol* **183**: 243–246
- Britto DT, Siddiqi MY, Glass AD, Kronzucker HJ (2001) Futile transmembrane NH<sub>4</sub><sup>+</sup> cycling: a cellular hypothesis to explain ammonium toxicity in plants. *Proc Natl Acad Sci USA* **98**: 4255–4258
- Caballero F, Botella MA, Rubio L, Fernández JA, Martínez V, Rubio F (2012) A Ca<sup>(2+)</sup>-sensitive system mediates low-affinity K<sup>(+)</sup> uptake in the absence of AKT1 in Arabidopsis plants. *Plant Cell Physiol* **53**: 2047–2059
- Cheeseman JM (2013) The integration of activity in saline environments: problems and perspectives. *Funct Plant Biol (in press)*
- Chérel I (2004) Regulation of K<sup>+</sup> channel activities in plants: from physiological to molecular aspects. *J Exp Bot* **55**: 337–351
- Coskun D, Britto DT, Jean YK, Schulze LM, Becker A, Kronzucker HJ (2012) Silver ions disrupt K<sup>+</sup> homeostasis and cellular integrity in intact barley (*Hordeum vulgare* L.) roots. *J Exp Bot* **63**: 151–162
- Coskun D, Britto DT, Kronzucker HJ (2010) Regulation and mechanism of potassium release from barley roots: an in planta <sup>42</sup>K<sup>+</sup> analysis. *New Phytol* **188**: 1028–1038
- Cuin TA, Miller AJ, Laurie SA, Leigh RA (2003) Potassium activities in cell compartments of salt-grown barley leaves. *J Exp Bot* **54**: 657–661
- Demidchik V, Davenport RJ, Tester M (2002) Nonselective cation channels in plants. *Annu Rev Plant Biol* **53**: 67–107
- Epstein E, Rains DW, Elzam OE (1963) Resolution of dual mechanisms of potassium absorption by barley roots. *Proc Natl Acad Sci USA* **49**: 684–692
- Essah PA, Davenport R, Tester M (2003) Sodium influx and accumulation in Arabidopsis. *Plant Physiol* **133**: 307–318
- Fu HH, Luan S (1998) AtKuP1: a dual-affinity K<sup>+</sup> transporter from Arabidopsis. *Plant Cell* **10**: 63–73
- Fuchs I, Stölzle S, Ivashikina N, Hedrich R (2005) Rice K<sup>+</sup> uptake channel OsAKT1 is sensitive to salt stress. *Planta* **221**: 212–221
- Fulgenzi FR, Peralta ML, Mangano S, Danna CH, Vallejo AJ, Puigdomenech P, Santa-María GE (2008) The ionic environment controls the contribution of the barley HvHAK1 transporter to potassium acquisition. *Plant Physiol* **147**: 252–262
- Garcia-deblás B, Senn ME, Bañuelos MA, Rodríguez-Navarro A (2003) Sodium transport and HKT transporters: the rice model. *Plant J* **34**: 788–801
- Geiger D, Becker D, Vosloh D, Gambale F, Palme K, Rehers M, Anshuetz U, Dreyer I, Kudla J, Hedrich R (2009) Heteromeric AtKCl1·AKT1 channels in Arabidopsis roots facilitate growth under K<sup>+</sup>-limiting conditions. *J Biol Chem* **284**: 21288–21295
- Gierth M, Mäser P (2007) Potassium transporters in plants: involvement in K<sup>+</sup> acquisition, redistribution and homeostasis. *FEBS Lett* **581**: 2348–2356
- Gierth M, Mäser P, Schroeder JI (2005) The potassium transporter AtHAK5 functions in K<sup>+</sup> deprivation-induced high-affinity K<sup>+</sup> uptake and AKT1 K<sup>+</sup> channel contribution to K<sup>+</sup> uptake kinetics in Arabidopsis roots. *Plant Physiol* **137**: 1105–1114
- Glass ADM (1976) Regulation of potassium absorption in barley roots: an allosteric model. *Plant Physiol* **58**: 33–37
- Goff SA, Ricke D, Lan TH, Presting G, Wang RL, Dunn M, Glazebrook J, Sessions A, Oeller P, Varma H, et al (2002) A draft sequence of the rice genome (*Oryza sativa* L. ssp. *japonica*). *Science* **296**: 92–100
- Grefen C, Chen Z, Honsbein A, Donald N, Hills A, Blatt MR (2010) A novel motif essential for SNARE interaction with the K<sup>+</sup> channel KCl1 and channel gating in Arabidopsis. *Plant Cell* **22**: 3076–3092
- Guerin M, Wallon G (1979) The reversible replacement of internal potassium by caesium in isolated turtle heart. *J Physiol* **293**: 525–537
- Hajibagheri MA, Flowers TJ, Collins JC, Yeo AR (1988) A comparison of the methods of x-ray-microanalysis, compartmental analysis and longitudinal ion profiles to estimate cytoplasmic ion concentrations in 2 maize varieties. *J Exp Bot* **39**: 279–290
- Halperin SJ, Lynch JP (2003) Effects of salinity on cytosolic Na<sup>+</sup> and K<sup>+</sup> in root hairs of Arabidopsis thaliana: in vivo measurements using the fluorescent dyes SBFI and PBFI. *J Exp Bot* **54**: 2035–2043
- Hampton CR, Bowen HC, Broadley MR, Hammond JP, Mead A, Payne KA, Pritchard J, White PJ (2004) Cesium toxicity in Arabidopsis. *Plant Physiol* **136**: 3824–3837
- Hille B (2001) Ion Channels of Excitable Membranes, Ed 3. Sinauer Associates, Sunderland, MA
- Hirsch RE, Lewis BD, Spalding EP, Sussman MR (1998) A role for the AKT1 potassium channel in plant nutrition. *Science* **280**: 918–921
- Honsbein A, Sokolovski S, Grefen C, Campanoni P, Pratelli R, Paneque M, Chen ZH, Johansson I, Blatt MR (2009) A tripartite SNARE-K<sup>+</sup> channel complex mediates in channel-dependent K<sup>+</sup> nutrition in Arabidopsis. *Plant Cell* **21**: 2859–2877
- Horie T, Costa A, Kim TH, Han MJ, Horie R, Leung HY, Miyao A, Hirochika H, An G, Schroeder JI (2007) Rice OsHKT2;1 transporter mediates large Na<sup>+</sup> influx component into K<sup>+</sup>-starved roots for growth. *EMBO J* **26**: 3003–3014
- Jeanguenin L, Alcon C, Duby G, Boeglin M, Chérel I, Gaillard I, Zimmermann S, Sentenac H, Véry AA (2011) AtKCl1 is a general modulator of Arabidopsis inward Shaker channel activity. *Plant J* **67**: 570–582
- Jeschke WD, Jambor W (1981) Determination of unidirectional sodium fluxes in roots of intact sunflower seedlings. *J Exp Bot* **32**: 1257–1272
- Kielland J (1937) Individual activity coefficients of ions in aqueous solutions. *J Am Chem Soc* **59**: 1675–1678
- Kim EJ, Kwak JM, Uozumi N, Schroeder JI (1998) AtKUP1: an Arabidopsis gene encoding high-affinity potassium transport activity. *Plant Cell* **10**: 51–62
- Kochian LV, Lucas WJ (1982) Potassium transport in corn roots. I. Resolution of kinetics into a saturable and linear component. *Plant Physiol* **70**: 1723–1731
- Kochian LV, Lucas WJ (1993) Can K<sup>+</sup> channels do it all? *Plant Cell* **5**: 720–721
- Kochian LV, Xin-Zhi J, Lucas WJ (1985) Potassium transport in corn roots. IV. Characterization of the linear component. *Plant Physiol* **79**: 771–776
- Krol E, Trebacz K (2000) Ways of ion channel gating in plant cells. *Ann Bot (Lond)* **86**: 449–469
- Kronzucker HJ, Britto DT (2011) Sodium transport in plants: a critical review. *New Phytol* **189**: 54–81
- Kronzucker HJ, Siddiqi MY, Glass ADM (1995) Analysis of <sup>13</sup>NH<sub>4</sub><sup>+</sup> efflux in spruce roots: a test case for phase identification in compartmental analysis. *Plant Physiol* **109**: 481–490
- Kronzucker HJ, Szczerba MW, Britto DT (2003) Cytosolic potassium homeostasis revisited: <sup>42</sup>K-tracer analysis reveals set-point variations in [K<sup>+</sup>]. *Planta* **217**: 540–546
- Kronzucker HJ, Szczerba MW, Moazami-Goudarzi M, Britto DT (2006) The cytosolic Na<sup>+</sup>:K<sup>+</sup> ratio does not explain salinity-induced growth impairment in barley: a dual-tracer study using <sup>42</sup>K<sup>+</sup> and <sup>24</sup>Na<sup>+</sup>. *Plant Cell Environ* **29**: 2228–2237
- Lagarde D, Basset M, Lepetit M, Conejero G, Gaymard F, Astruc S, Grignon C (1996) Tissue-specific expression of Arabidopsis AKT1 gene is consistent with a role in K<sup>+</sup> nutrition. *Plant J* **9**: 195–203
- Lazof D, Cheeseman JM (1986) Sodium transport and compartmentation in *Spergularia marina*: partial characterization of a functional symplast. *Plant Physiol* **81**: 742–747

- Lee KS, Tsien RW (1983) Mechanism of calcium channel blockade by verapamil, D600, diltiazem and nitrendipine in single dialysed heart cells. *Nature* **302**: 790–794
- Lee RB, Clarkson DT (1986) Nitrogen-13 studies of nitrate fluxes in barley roots. 1. Compartmental analysis from measurements of  $^{13}\text{N}$  efflux. *J Exp Bot* **37**: 1753–1767
- Lee SC, Lan WZ, Kim BG, Li L, Cheong YH, Pandey GK, Lu G, Buchanan BB, Luan S (2007) A protein phosphorylation/dephosphorylation network regulates a plant potassium channel. *Proc Natl Acad Sci USA* **104**: 15959–15964
- Leigh RA, Wyn-Jones RG (1984) A hypothesis relating critical potassium concentrations for growth to the distribution and functions of this ion in the plant cell. *New Phytol* **97**: 1–13
- Li L, Kim BG, Cheong YH, Pandey GK, Luan S (2006) A  $\text{Ca}^{2+}$  signaling pathway regulates a  $\text{K}^+$  channel for low-K response in *Arabidopsis*. *Proc Natl Acad Sci USA* **103**: 12625–12630
- Ling GN (1969) Measurement of potassium ion activity in the cytoplasm of living cells. *Nature* **221**: 386–387
- Maathuis FJM, Sanders D (1993) Energization of potassium uptake in *Arabidopsis thaliana*. *Planta* **191**: 302–307
- Maathuis FJM, Sanders D (1994) Mechanism of high-affinity potassium uptake in roots of *Arabidopsis thaliana*. *Proc Natl Acad Sci USA* **91**: 9272–9276
- Maathuis FJM, Sanders D (1996) Mechanisms of potassium absorption by higher plant roots. *Physiol Plant* **96**: 158–168
- Malhotra B, Glass ADM (1995) Potassium fluxes in *Chlamydomonas reinhardtii*. I. Kinetics and electrical potentials. *Plant Physiol* **108**: 1527–1536
- Mayer KFX, Waugh R, Brown JW, Schulman A, Langridge P, Platzer M, Fincher GB, Muehlbauer GJ, Sato K, Close TJ, et al (2012) A physical, genetic and functional sequence assembly of the barley genome. *Nature* **491**: 711–716
- Memon AR, Saccomani M, Glass ADM (1985) Efficiency of potassium utilization by barley varieties: the role of subcellular compartmentation. *J Exp Bot* **36**: 1860–1876
- Nocito FF, Sacchi GA, Cocucci M (2002) Membrane depolarization induces  $\text{K}^+$  efflux from subapical maize root segments. *New Phytol* **154**: 45–51
- Palmer LG, Century TJ, Civan MM (1978) Activity coefficients of intracellular  $\text{Na}^+$  and  $\text{K}^+$  during development of frog oocytes. *J Membr Biol* **40**: 25–38
- Poole RJ (1971) Effect of sodium on potassium fluxes at the cell membrane and vacuole membrane of red beet. *Plant Physiol* **47**: 731–734
- Pyo YJ, Gieth M, Schroeder JI, Cho MH (2010) High-affinity  $\text{K}^+$  transport in *Arabidopsis*: AtHAK5 and AKT1 are vital for seedling establishment and postgermination growth under low-potassium conditions. *Plant Physiol* **153**: 863–875
- Qi Z, Hampton CR, Shin R, Barkla BJ, White PJ, Schachtman DP (2008) The high affinity  $\text{K}^+$  transporter AtHAK5 plays a physiological role in planta at very low  $\text{K}^+$  concentrations and provides a caesium uptake pathway in *Arabidopsis*. *J Exp Bot* **59**: 595–607
- Robinson RA, Stokes RH (1965) *Electrolyte Solutions*, Ed 2. Butterworth, London
- Rubio F, Alemán F, Nieves-Cordones M, Martínez V (2010) Studies on *Arabidopsis* athak5, atakt1 double mutants disclose the range of concentrations at which AtHAK5, AtAKT1 and unknown systems mediate K uptake. *Physiol Plant* **139**: 220–228
- Rubio F, Gassmann W, Schroeder JI (1995) Sodium-driven potassium uptake by the plant potassium transporter HKT1 and mutations conferring salt tolerance. *Science* **270**: 1660–1663
- Rubio F, Nieves-Cordones M, Alemán F, Martínez V (2008) Relative contribution of AtHAK5 and AtAKT1 to  $\text{K}^+$  uptake in the high-affinity range of concentrations. *Physiol Plant* **134**: 598–608
- Santa-María GE, Danna CH, Czibener C (2000) High-affinity potassium transport in barley roots: ammonium-sensitive and -insensitive pathways. *Plant Physiol* **123**: 297–306
- Santa-María GE, Rubio F, Dubcovsky J, Rodríguez-Navarro A (1997) The HAK1 gene of barley is a member of a large gene family and encodes a high-affinity potassium transporter. *Plant Cell* **9**: 2281–2289
- Schulze LM, Britto DT, Li M, Kronzucker HJ (2012) A pharmacological analysis of high-affinity sodium transport in barley (*Hordeum vulgare* L.): a  $^{24}\text{Na}^+ / ^{42}\text{K}^+$  study. *J Exp Bot* **63**: 2479–2489
- Siddiqi MY, Glass ADM (1986) A model for the regulation of  $\text{K}^+$  influx, and tissue potassium concentrations by negative feedback effects upon plasmalemma influx. *Plant Physiol* **81**: 1–7
- Siddiqi MY, Glass ADM, Ruth TJ (1991) Studies of the uptake of nitrate in barley. 3. Compartmentation of  $\text{NO}_3^-$ . *J Exp Bot* **42**: 1455–1463
- Spalding EP, Hirsch RE, Lewis DR, Qi Z, Sussman MR, Lewis BD (1999) Potassium uptake supporting plant growth in the absence of AKT1 channel activity: inhibition by ammonium and stimulation by sodium. *J Gen Physiol* **113**: 909–918
- Subbarao GV, Ito O, Berry WL, Wheeler RM (2003) Sodium: a functional plant nutrient. *Crit Rev Plant Sci* **22**: 391–416
- Szczerba MW, Britto DT, Balkos KD, Kronzucker HJ (2008) Alleviation of rapid, futile ammonium cycling at the plasma membrane by potassium reveals  $\text{K}^+$ -sensitive and -insensitive components of  $\text{NH}_4^+$  transport. *J Exp Bot* **59**: 303–313
- Szczerba MW, Britto DT, Kronzucker HJ (2009)  $\text{K}^+$  transport in plants: physiology and molecular biology. *J Plant Physiol* **166**: 447–466
- ten Hoopen F, Cuin TA, Pedas P, Hegelund JN, Shabala S, Schjoerring JK, Jahn TP (2010) Competition between uptake of ammonium and potassium in barley and *Arabidopsis* roots: molecular mechanisms and physiological consequences. *J Exp Bot* **61**: 2303–2315
- Ullrich WR, Larsson M, Larsson CM, Lesch S, Novacky A (1984) Ammonium uptake in *Lemna gibba* G1, related membrane potential changes, and inhibition of anion uptake. *Physiol Plant* **61**: 369–376
- Vale FR, Jackson WA, Volk RJ (1987) Potassium influx into maize root systems: influence of root potassium concentration and ambient ammonium. *Plant Physiol* **84**: 1416–1420
- Vallejo AJ, Peralta ML, Santa-María GE (2005) Expression of potassium-transporter coding genes, and kinetics of rubidium uptake, along a longitudinal root axis. *Plant Cell Environ* **28**: 850–862
- Véry AA, Sentenac H (2003) Molecular mechanisms and regulation of  $\text{K}^+$  transport in higher plants. *Annu Rev Plant Biol* **54**: 575–603
- Walker DJ, Leigh RA, Miller AJ (1996) Potassium homeostasis in vacuolate plant cells. *Proc Natl Acad Sci USA* **93**: 10510–10514
- Walker NA, Pitman MG (1976) Measurement of fluxes across membranes. In U Luetge, MG Pitman, eds, *Encyclopedia of Plant Physiology*, Vol 2. Springer-Verlag, Berlin, pp 93–126
- Wang MY, Glass ADM, Shaff JE, Kochian LV (1994) Ammonium uptake by rice roots. III. Electrophysiology. *Plant Physiol* **104**: 899–906
- White PJ (1998) Calcium channels in the plasma membrane of root cells. *Ann Bot (Lond)* **81**: 173–183
- White PJ, Broadley MR (2000) Mechanisms of caesium uptake by plants. *New Phytol* **147**: 241–256
- White PJ, Davenport RJ (2002) The voltage-independent cation channel in the plasma membrane of wheat roots is permeable to divalent cations and may be involved in cytosolic  $\text{Ca}^{2+}$  homeostasis. *Plant Physiol* **130**: 1386–1395
- White PJ, Earnshaw MJ, Clarkson DT (1991) Effects of growth and assay temperatures on unidirectional  $\text{K}^+$  fluxes in roots of rye (*Secale cereale*). *J Exp Bot* **42**: 1031–1041
- White PJ, Lemtiri-Chlieh F (1995) Potassium currents across the plasma membrane of protoplasts derived from rye roots: a patch-clamp study. *J Exp Bot* **46**: 497–511
- Xu J, Li HD, Chen LQ, Wang Y, Liu LL, He L, Wu WH (2006) A protein kinase, interacting with two calcineurin B-like proteins, regulates  $\text{K}^+$  transporter AKT1 in *Arabidopsis*. *Cell* **125**: 1347–1360
- Yu J, Hu SN, Wang J, Wong GKS, Li SG, Liu B, Deng YJ, Dai L, Zhou Y, Zhang XQ, et al (2002) A draft sequence of the rice genome (*Oryza sativa* L. ssp. *indica*). *Science* **296**: 79–92
- Zhang JL, Flowers TJ, Wang SM (2010) Mechanisms of sodium uptake by roots of higher plants. *Plant Soil* **236**: 45–60